DEUTSCHES ELEKTRONEN-SYNCHROTRON DESY

DESY 69/22
July 1969

Electroproduction of $N^*(1236)$ in a Ladder Approximation Model

by

Fritz Gutbrod

2 HAMBURG 52 · NOTKESTIEG 1

Electroproduction of $N^*(1236)$ in a Ladder Approximation Model

by

Fritz Gutbrod

Abstract

Electroproduction of $N^*(1236)$ is described by a model, in which the left hand cut of the pion production multipoles is approximated by the sum of ladder diagrams containing nucleon and pion exchange with cut-offs. The cut-off parameters have been fixed by use of scattering and photoproduction data. Taking the cut-offs independent of the virtual photon four momentum, predictions for the two transverse multipoles and for the scalar multipole are given. Special emphasis is laid on a discussion of the resonance shape for different momentum transfer.

I. Introduction

In this paper we want to describe the $N^*(1236)$ as a resonant state of pion and nucleon by means of the Bethe-Salpeter equation in ladder approximation, with the interaction given by nucleon exchange. Especially we are interested into the electromagnetic excitation of this resonance, exploring some detailed questions such as the magnitude of the small multipoles and the variation of the resonance shape with varying momentum transfer in pion electroproduction. To look at as many details of that process as possible is motivated by the fact that in a description of the resonance by the Bethe-Salpeter technique some parameters have to be introduced, the first one being a cut-off in the nucleon exchange potential, which may be fixed by the requirement that the resonance appears at the experimental position. Then the Bethe-Salpeter wave function of the N^* is determined, and it can be checked by calculating electromagnetic transition matrix elements. For this purpose we have to make the additional assumption that the transition potential * leading from the state γN to πN can be approximated by nucleon and pion exchange diagrams shown in Fig.1, where the bubbles at the photon vertices indicate the insertion of electromagnetic form factors. The diagrams should also be modified by cut-offs. Therefore only a successful description of all three multipoles (magnetic, electric and scalar or longitudinal), both in energy and momentum transfer dependence, by such a transition potential would be a satisfactory check of the model.

Our interest into the resonance shape comes from the fact that the resonance lies close to the πN-threshold, in which region the transition potentials change their energy dependence strongly for different photon masses. Since the resonance width is comparable to its distance to the threshold we may expect interesting effects on the resonance shape.

---

*By potential we mean a set of two particle irreducible, partial wave projected diagrams.

Such effects have already been predicted by dispersion theoretical treatments of the electroproduction problem.[1-5] For instance the authors of Refs. (4) and (5) have proposed as a reasonable solution of dispersion relations

$$M(W, k^2) \approx M^{Born}(W, k^2) \cdot f(W) \qquad (1)$$

where $M(W, k^2)$ is a multipole amplitude, $M^{Born}(W,k^2)$ denotes the Born approximation of the dominant nucleon exchange part of the transion potential, $f(W)$ contains the resonance dependence on the CM-energy W, and k^2 is the photon four momentum squared. Those parts of the transition amplitude coming from pion exchange are not expected to obey Eq.(1) because of their different energy dependence,[2] and their treatment is certainly more involved.

The present experimental data[6,7] are not in good agreement with Eq.(1) as can be seen from the analysis of Adler[2] whose predictions for the k^2-dependence fall above that of Eq.(1) but are too low experimentally.* Since there exists also no quantitative justification of that approximation, we consider it worthwhile to reexamine the problem of the energy dependence together with that of the k^2-dependence.

As an alternative method to dispersion theory it would be desirable to solve the Bethe-Salpeter equation (BSE) for the πNN^* vertex, and to calculate the electroexitation of the N^* from the diagrams of Fig.2 . Since there are extreme difficulties due to the many different masses in that process we have preferred a procedure which uses partly dispersion techniques: The BSE will be iterated for values of the CMS-energy W on a complex contour C_W separating the right hand and left hand cut in the W-plane of the multipole amplitudes (Fig.3). By the Cauchy formula we thus get a perturbation expansion of the left hand cut contribution to these amplitudes

*Of course one might take this as a hint for the contributions from other one particle exchange graphs,[5] especially ω-exchange. We believe however that Eq.(1) is not reliable (see Section 6 for a detailed discussion).

which has been shown to converge quite rapidly if the cut-off for the exchanged nucleon is choosen properly.[8] The construction of the complete amplitude is then easily accomplished by means of the Omnès-Mushelishvili-method.[9] A disadvantage of this procedure is that we combine an experimental phase shift with the left hand cut of a model amplitude which may yield a resonance at a slightly different position. A direct solution of the BSE in the resonance region is therefore unavoidable and will be attempted later.

In Section 2 we describe the technical details of the computation of ladder diagrams respectively their left hand cut, and specify the cut-off in the nucleon exchange potential. In Section 3 the electromagnetic transition potential will be discussed, and its cut-off parameters are determined from a comparison with photoproduction data. In addition we discuss in the frame work of the nonrelativistic Lippman-Schwinger equation the effects that arise when transition potential and interaction potential have very different ranges. This discussion should help to understand such phenomena as zeros in multipole amplitudes in a more transparent way than the present dispersion language offers.
Section 4 contains the prediction for the magnetic dipole in electroproduction with an emphasis on the variation of the resonance shape. The agreement of the predicted magnetic form factor with experimental data[7] is not very good, if the assumption is made, that the pion electromagnetic form factor is equal to the nucleon electric (Sachs) form factor. If the pion form factor however shows ρ-dominance, the experiments are reproduced satisfactorily. In the same section the predictions for the small multipoles (electric and scalar quadrupole) are presented. In Section 5 we try to compare the various methods used in dispersion theory with our approach.

II. Calculation of Ladder Diagrams

We assume the pion electroproduction amplitudes $M(W,k^2)$ (where M stands for all relevant multipoles) to be determined by the two component Bethe-Salpeter equation (graphically represented in Fig.4)

$$M_i(q_o,|\vec{q}|) = M_i^{Born}(q_o,|\vec{q}|) - \frac{i}{\pi^2}\int dq_o' d|\vec{q}'|\sum_{j=1,2} K_{ij}(q_o,|\vec{q}|,q_o',|\vec{q}'|)\times$$

$$i = 1,2 \qquad \times M_j(q_o',|\vec{q}'|)\ , \qquad (2)$$

with * $M(W,k^2) = M_1(p_o,|\vec{p}|)$.

Here $M_i^{Born}(q_o,|\vec{q}|)$ denotes the projections of the nucleon and pion exchange diagrams of Fig.1 into the appropriate multipole channel as a function of the final off-shell pion-nucleon relative energy q_o and relative momentum $|\vec{q}|$. These functions will be given in Appendix A. The interaction kernel $K_{ij}(q_o,|\vec{q}|, q_o',|\vec{q}'|)$, which is responsible for the formation of the resonance, is for elementary nucleon exchange given by[8]

$$K_{ij}(q_o,|\vec{q}|, q_o',|\vec{q}'|) = \frac{g^2}{4\pi}\frac{|\vec{q}'|}{|\vec{q}|}\frac{\alpha_i}{\left((q_o'+\frac{W}{2})^2-\vec{q}'^2-\mu^2\right)\left(q_o'-\frac{W}{2}\right)^2-\vec{q}'^2-M^2)}\times$$

$$\times\{(q_o+q_o'+r_i+r_j'-M)\sqrt{r_i+M}\ \sqrt{r_j'+M}\ Q_1(Z)$$

$$+\ (q_o+q_o'+r_i+r_j'+M)\sqrt{r_i-M}\ \sqrt{r_j'-M}\ Q_2(Z)\}\ ,$$

$$\text{with } \frac{g^2}{4\pi} = 14.5\ , \qquad (3)$$

$$r_1 = -r_2 = \sqrt{\vec{q}^{\,2}+M^2},$$

$$r_1' = -r_2' = \sqrt{\vec{q}'^2+M^2},$$

*By p_o , $\vec{p}$ we denote on-shell relative energy and three momentum of nucleon and pion. The arguments W and k^2 have been omitted in $M_i(q_o,|\vec{q}|)$.

$$\alpha_1 = 1 - \alpha_2 = \frac{1}{2}\left(1 + \frac{W - 2q'_o}{2r'_1}\right) ,$$

$$Z = \{(q_o + q'_o)^2 - \vec{q}^2 - \vec{q}'^2 - M^2\}/2|\vec{q}||\vec{q}'| ,$$

M = nucleon mass,

μ = pion mass,

and $Q_\ell(Z)$ = Legendre-functions of second kind.

Other kinematical quantities are:

k_o = photon CMS energy,

$|\vec{k}|$ = photon CMS three momentum .

If we modify the propagator of the exchanged nucleon by a form factor of a simple pole type (u being the four momentum squared of the exchanged nucleon),

$$\frac{1}{u - M^2} \Rightarrow \frac{1}{u - M^2} \cdot \frac{1}{1 - \frac{u - M^2}{\Lambda^2}} = \frac{1}{u - M^2} - \frac{1}{u - M^2 - \Lambda^2} \qquad (4)$$

which may represent a combination of propagator and vertex corrections and is of purely phenomenological nature presently, we have to modify expression (3) by the substitution

$$Q_\ell(Z) \Rightarrow Q_\ell(Z) - Q_\ell(Z') \qquad (5)$$

$$Z' = Z - \Lambda^2/2|\vec{q}||\vec{q}'| \quad .$$

An estimate of the cut-off parameter Λ^2 has been obtained in Ref.8 by an evaluation of a dispersion sum rule for the elastic πN scattering amplitude in the (3,3)-channel, $f_{1+}(W)$, in comparison with the ladder approximation for the left hand cut of $f_{1+}(W)$. A value of $\Lambda^2 = 2.6$ GeV^2 yields a reasonable left hand cut.

Eq.(2) has been iterated by numerical integration for values of W varying along the complex contour C_W of Fig.3 which has been choosen lying far from the positive W-axis. We thus get an expansion of the transition amplitude into powers of the strong coupling constant $g^2/4\pi$, which enables us to calculate the ladder series for the left hand cut of the multipole amplitudes $M(W,k^2)$ by the Cauchy formula

$$M_L(W,k^2) = \frac{1}{2\pi i} \int_{C_W} dW' \frac{\sum_{n=0} M^{(n)}(W',k^2)}{W' - W} \quad , \tag{6}$$

where $M^{(n)}(W,k^2)$ denotes the n-th iteration of Eq.(2) with

$$M^{(0)}(W,k^2) = M^{Born}(W,k^2) \quad . \tag{7}$$

Our choice of the contour C_W is motivated by the consideration that it should stay far away from the real W-axis, where the convergence of the series in the integrand of Eq.(6) is bad due to the resonance pole, since this would lead to large cancellations along the integration path (the integrated series converges quite rapidly).[8]

It has been shown in Ref.(8) that the use of complex values of W also helps to separate the various singularities of the kernel and of the inhomogeneous term in Eq.(2) with respect to the q_o-variable, which for real W make a numerical iteration difficult beyond the inelastic threshold $W_{in} = M + 2\mu$. The small pion mass however in the pion exchange diagram Fig.1b) causes additional difficulties in the following way: The Born term $M_i^{Born}(q_o', |\vec{q}'|)$ has cuts in the q_o'-variable starting at *

$$q_o' = k_o - \frac{W}{2} \pm \sqrt{(|\vec{q}'| \pm |\vec{k}|)^2 + \mu^2} \quad . \tag{8}$$

*Unfortunately the quantities $|\vec{k}|, |\vec{q}'|$ etc. are not necessarily real here due to the complex values of W .

If in the course of the $|\vec{q}'|$-integration in Eq.(2) we arrive at

$$\mathrm{Re}|\vec{q}'| = \mathrm{Re}|\vec{k}|$$

we must have

$$\left|\mathrm{Im}(|\vec{q}'| - |\vec{k}|)\right| < \mu \tag{9}$$

in order to retain a real gap for the complex q_o'-integration. The contour of the $|\vec{q}'|$-integration has to be deformed from the real axis as to fullfil condition (9). The actual contour was taken as

$$|\vec{q}'| = \begin{cases} \lambda(|\vec{k}| - i\frac{\mu}{2}) , & 0 \le \lambda \le 1 \\ |\vec{k}| - i\frac{\mu}{2} + \lambda, & 0 \le \lambda < \infty \end{cases} .$$

Now if $|\vec{k}| \approx |\vec{p}|$ two of the four poles contained in the propagators in K_{ij} approach each other again closely, since for $|\vec{q}'| = |\vec{p}| - i\frac{\mu}{2}$ they lay at

$$q_{o1}' = -\frac{W}{2} + \sqrt{|\vec{q}'|^2 + \mu^2} ,$$

$$q_{o2}' = \frac{W}{2} - \sqrt{|\vec{q}'|^2 - M^2}$$

$$\approx q_{o1}' + i\frac{\mu}{2} ,$$

if $|\vec{q}'|^2 >> \mu^2$.

The pinching of the q_o'-integration contour by these poles, which of course corresponds to the well known two particle singularities of $M(W,k^2)$, causes a pole in the $|\vec{q}'|$-integration at $|\vec{q}'| = |\vec{p}|$, the contribution of which was subtracted numerically and added again analytically in a standard manner. The same was done for the single poles in q_o' which cross the q_o'-contour for increasing $|\vec{q}'|$ after the Wick rotation has been performed. For large k^2 however there is no gap between the cuts (8) from

pion exchange and the cuts coming from elastic scattering nucleon exchange, (which are located at

$$q_o' = - p_o \pm \sqrt{(|\vec{q}'| \pm |\vec{p}|)^2 + M^2} \quad) \,, \tag{10}$$

which is opened for all values of $|\vec{q}'|$. This could be managed by using a q_o'-integration contour which depends on $|\vec{q}'|$, but we have preferred to use a contour going through the gap between the cuts of Eq.(10) and to extrapolate the amplitude in q_o' when doing the integration over the pion Born terms. For this reason we have restricted the present calculations to the region $|k^2| < 1 (GeV/c)^2$.

The numerical integration was performed with Gaussian quadrature taking 11 points for the $|\vec{q}'|$-integration and 14-20 for the q_o'-integration. For the calculations an IBM 360-75 was available.

In order to improve the convergence of the perturbation expansion in Eq.(6), the diagonal Pade approximants[10] have been formed from the ladder diagrams $M^{(n)}(W,k^2)$, thus actually calculating

$$M_{L,N}(W,k^2) \equiv \frac{1}{2\pi i} \int_{C_W} dW' \, \frac{[M(W',k^2)]_{N,N}}{W' - W} \tag{11}$$

with $N = 2$ or $N = 3$. The differences between M_L as defined in Eq.(6), between $M_{L,2}$ and $M_{L,3}$ were of the order of 3% for all W . The calculations reported were mainly done using the [2,2] - approximant, which requires ladders with four rungs.

Given the left hand cut of our multipole amplitude $M(W,k^2)$ and the scattering phase shift $\delta(W)$ for all energies and assuming elastic unitarity, the complete amplitude with the correct phase, and prescribed left hand and the correct threshold behavior is [9]

$$M(W,k^2) = M_L(W,k^2) - \frac{\rho(W,k^2)}{\pi D(W)} \int_{M+\mu}^{\infty} dW' \frac{\mathrm{Im}\, D(W')}{W' - W - i\varepsilon} \times \tag{12a}$$

$$\times \{M(W',k^2)/\rho(W',k^2)\}_{\text{left h.c.}}$$

$$\approx \frac{\rho(W,k^2)}{2\pi i D(W)} \int_{C_W} dW' \frac{D(W')[M(W',k^2)]_{N,N}}{\rho(W',k^2)(W' - W)} \quad , \tag{12b}$$

$$\text{with } D(W) = \exp\left\{ - \frac{W-M}{\pi} \int_{M+\mu}^{\infty} dW' \frac{\delta(W')}{(W'-M)(W'-W-i\varepsilon)} \right\}, \tag{12c}$$

$$\text{and } \rho(W,k^2) = |\vec{p}|\,|\vec{k}|\, W \sqrt{E_1 + M}\, \sqrt{E_2 + M} \quad ,$$

where

E_1 = CMS - energy of incoming nucleon,

E_2 = CMS - energy of outgoing nucleon.

This form of the amplitude is unique even if $\delta(\infty) \neq 0$ due to asymptotic considerations. Formally one may add to Eq.(12) a homogenous term

$$M(W,k^2)_{\text{hom}} = \text{const} \frac{\rho(W,k2)}{D(W)} \tag{13}$$

which does not disturb the phase and the left hand cut of (12), but it has an asymptotic behavior which is inconsistent with unitarity, and no cancellations can occur between Eqs.(12) and (13), since $M(W,k^2)_{\text{hom}}$ decreases at least one power slower in W than the solution of Eq.(12). We have to

be aware of the fact, however, that the actual function defined by (12) generally will violate unitarity also due to imperfecties in $M_L(W,k^2)$ and due to a breakdown of elastic unitarity. Nevertheless it is the only form of the amplitude which may have the correct asymtotics. Neglection of asymtotic behavior certainly allows for addition of terms like (13).[11]

Our choice of the kinematical function $\rho(W,k^2)$ ensures the correct threshold behavior and helps to reduce the high energy region contribution in Eq.(12) where the calculation of ladder diagrams becomes imprecise. The results for $M(W,k^2)$ should not depend on the special choice of $\rho(W,k^2)$, but they do in practice. This is of course due to our technique to calculate the left hand cut from the BSE with a cut-off parameter determined to reproduce that quantity at infinity, while our phase shift is taken from experiment and may not coincide with that following from the BSE. The deviations of $M(W,k^2)$ for choices of $\rho(W,k^2)$ differing by a power of W are of the order of 10% in the resonance region.

The phase shift $\delta(W)$ was taken as an interpolation to the data of Donnachie et al.,[12] and it was extrapolated to $\pi/2$ at infinity. A recalculation of the scattering amplitude by the same technique as described for the multipoles gave back the input amplitude as determined by the phase shift up to 15% below $W = 9.5\mu$.

Having described the details of our calculation technique, we turn to a determination of the parameters of the transition potential, which we approximate by single particle exchange forces with form factors both with respect to the electromagnetic and to the strong vertices.

III. The $\gamma N \to \pi N$ Transition Potential

For the scattering amplitude the need for a cut-off in the propagator of the exchanged nucleon is obvious, since with an unmodified propagator the ladder series for the left hand cut does not converge,[8] and in a numerical solution[13] of the BSE the N^* appears for $g^2/4\pi = 10$ as a bound state. The electroproduction amplitudes can in principle be calculated without a

cut-off in the one-particle exchange diagrams of Fig.1) from Eq.(2), but if we interprete the cut-off as a combination of vertex and self-energy corrections we would expect approximately the same cut-off for diagram Fig.1a) as for the scattering diagram. For the pion exchange diagram Fig.1b) we have to assume another cut-off for the pion-nucleon vertex and for the pion propagator. Thus we modify

$$\frac{1}{u - M^2} \Rightarrow \frac{1}{u - M^2} - \frac{1}{u - M^2 - \Lambda_N^2} \qquad \text{in Fig.1a)} \tag{14}$$

and

$$\frac{1}{t - \mu^2} \Rightarrow \frac{1}{t - \mu^2} - \frac{1}{t - \mu^2 - \Lambda_\pi^2} \qquad \text{in Fig.1b)} \tag{15}$$

and determine the parameters Λ_N^2 and Λ_π^2 from photoproduction data. As input we use the absolute normalization of the magnetic dipole amplitude $M_{1+}(W,0)$ around the resonance region $W = W_r$, and the observation that the electric quadropole has a zero in the resonance region, which follows from an analysis of photoproduction data by Schwela et al.[14] Since the precise position obtained for this zero is different for the analysis of π^+ and π^0-photoproduction and depends also on assumptions on other multipoles, we shall make the working hypothesis that it is located at W = 1280 MeV (Lab. photon energy = 400 MeV). Since for $\Lambda_N^2 < 3$ GeV^2 the nucleon exchange contribution to $E_{1+}(W,0)$ is small for $W \sim W_r$, we first investigate the energy dependence of $E_{1+}(W,0)$ as a function of Λ_π^2 for fixed $\Lambda_N^2 = \Lambda^2$, which is the most natural choice. In Fig.5 we plot the ratio

$$\frac{|\vec{p}|}{|\vec{k}|} \frac{E_{1+}(W,0)}{f_{1+}(W)}$$

for different choices of Λ_π^2, where both amplitudes are calculated from Eq.(12). For decreasing Λ_π^2 the position of the zero is seen to move to lower energies, and a value of

$$\Lambda_\pi^2 = 0.5 \text{ GeV}^2 \tag{16}$$

shifts it to $W = 1{,}270$ GeV. We shall keep this value of Λ_π^2 in the course of our further calculations and determine Λ_N^2 by the requirement[14]

$$\frac{|\vec{p}|}{|\vec{k}|} \frac{M_{1+}(W_r,0)}{f_{1+}(W_r)} \approx 0.051 \tag{17}$$

Fig.6) shows that a value of $\Lambda_N^2 = \Lambda^2 = 2.6$ GeV^2 reproduces this ratio very well.

The existence of a zero in $E_{1+}(W,0)$ close to W_r of course forces this amplitude to be very small in the resonance region. It is a matter of definition whether one interprctes this already as an almost vanishing E_{1+}-coupling of the γNN^*-vertex, or if one extracts this quantity from the radius of a circle in a Argand diagram of the amplitude. In Fig.7) we compare the Argand diagrams of $M_{1+}(W,0)$ and $E_{1+}(W,0)$ and find from the radii that the resonant contribution of E_{1+} is about 6% of M_{1+}, but it is out of phase by 90° and has a large nonresonant background.

The behavior of the E_{1+}-amplitude requires an heuristic interpretation. We shall discuss in Appendix B a nonrelativistic model of the photo-disintegration of a bound state leading to a final resonant state. We shall indicate how in the case of a broad resonance the disintegration amplitude is likely to develop a zero, if the range of the transition potential is much larger than the range of the scattering potential, which is responsible for the resonance. The energy behavior of a transition amplitude thus can give us a qualitative indication for the ranges of forces occuring in scattering and transition processes. The observed behavior of the E_{1+}-amplitude is the consequence of the dominating long range forces coming from pion exchange, the short range part being suppressed by the cut-off.

In dispersion theory a similar reasoning is possible,[2] when the range of the force is defined by the energy behavior of the on-shell transition potential. This will be shortly discussed in Section 5.

IV. Electroproduction Amplitudes

After having defined our transition potential by adjusting the parameters Λ_N^2 and Λ_π^2 in photoproduction, we can calculate the electroproduction amplitudes under the assumption that Λ_N^2 and Λ_π^2 do not depend on k^2. An equivalent assumption is that the photon vertices in Fig.1 depend on k^2 only in a multiplicative way, i.e. that the vertex is given by a function of the nucleon and pion off-shell momenta times the on-shell electromagnetic form factor.

a) Magnetic Dipole, Resonance Shape

We want to separate two effects which govern the variation of the resonance shape, in a somehow artificial way. The simplest approximation takes into account only the threshold behavior which states that

$$M(W,k^2) \approx \frac{|\vec{k}(W,k^2)|}{|\vec{k}(W,0)|} \; M(W,0) \cdot G^*(k^2) \tag{18}$$

where $|\vec{k}(W,k^2)|$ is the photon CMS three-momentum. Since this quantity varies by 50% over the resonance width for $k^2 = 0$ and is almost constant for $k^2 < -0.3\ (\mathrm{GeV/c})^2$ we clearly should see this effect experimentally.

This threshold behavior is expected to hold[15] if

$$|\vec{k}| \cdot R \ll 1$$

where R is the range of the transition potential.* Therefore the contributions from pion exchange will not follow Eq.(18) even for $|k^2| < 0.1\ (\mathrm{GeV/c})^2$, whereas the corrections for the nucleon exchange terms are moderate for $k^2 \approx -1(\mathrm{GeV/c})^2$. We illustrate these effects in Fig.8 where the ratio

*Usually the threshold behavior is mainly used to draw conclusions for the k^2-dependence of an amplitude, but the W-dependence can be guessed as well from (18).

$$R(W,k^2) = \frac{|\vec{k}(W,0)|}{|\vec{k}(W,k^2|} \frac{M_{1+}(W,k^2)}{M_{1+}(W,0)} \frac{G_M^p(0)}{G_M^p(k^2)} \tag{19}$$

is drawn.

The amplitudes M_{1+} have been calculated according to Eq.(12) with the following assumtpions on the nucleon and pion form factors:

$$F_\pi(k^2) = G_e^p(k^2) = \frac{G_M^p(k^2)}{\mu^p} = \frac{G_M^N(k^2)}{\mu^N} \tag{20}$$

and $G_E^N(k^2) = 0$.

For the highest k^2 $(-1(\mathrm{GeV/c})^2)$ the variation of $R(W,k^2)$ across the resonance width is 30%.

Most of this large effect is caused by the pion exchange contribution which can easily be understood as a consequence of the small pion mass. As has been pointed out in Appendix B, a transition potential of a range long compared to the scattering potential will easily lead to an amplitude with a zero. Now the "range" of the potential is also a function of the external masses. Let us study for scalar particles the contribution of a one particle exchange potential with mass μ to the ℓ-th partial wave:

$$M_\ell^{\mathrm{Born}} = \frac{\mathrm{const}}{2|\vec{k}||\vec{q}|} Q_\ell(Z) \quad , \tag{21}$$

$$Z = \left(\mu^2 + \vec{q}^2 + \vec{k}^2 - (q_o - k_o)^2\right)/2|\vec{k}||\vec{q}|$$

where for a moment we have denoted the four momentum of the final off-shell pion by $(q_o, \vec{q})$. Let us define, in a nonrelativistic approximation, the "range" by min $(1/|\vec{q}|)$, up to which the threshold behavior $M_\ell^{\mathrm{Born}} \sim |\vec{q}|^\ell$, is approximately valid for fixed q_o . Obviously a large k^2 has the same effect as a large μ^2 in the sence that the range of the potential increases for increasing negative k^2 . Consequently the pion exchange

part of the amplitude will shift its resonance peak to higher energies for large momentum transfer (see Appendix B). Important effects from the nucleon exchange part will occur only for

$$k^2 < -M^2$$

which is outside the region of our present calculations.

We want to compare our results with the simple formula (2) where M^{Born} is either the sum of nucleon and pion terms or the nucleon term alone. In Table I we have listed the ratios

$$R^{Born}_{N+\pi}(W,k^2) \equiv \frac{|\vec{k}(W,0)|}{|\vec{k}(W,k^2)|} \frac{M^{Born}_{1+,N}(W,k^2) + M^{Born}_{1+,\pi}(W,k^2)}{M^{Born}_{1+,N}(W,0) + M^{Born}_{1+,\pi}(W,0)} \frac{1}{G_E^p(k^2)} \tag{22}$$

and

$$R^{Born}_{N}(W,k^2) \equiv \frac{|\vec{k}(W,0)|}{|\vec{k}(W,k^2)|} \frac{M^{Born}_{1+,N}(W,k^2)}{M^{Born}_{1+,N}(W,0)} \frac{1}{G_E^p(k^2)} \tag{23}$$

and compared them with the quantity $R(W,k^2)$ defined in Eq.(19). Clearly Eq.(2) gives rather different results for the k^2-dependence of M_{1+} as compared to the Bethe-Salpeter model. If we normalize $R^{Born}_{N+\pi}(W,k^2)$ to $R(W,k^2)$ at $W = 9\mu$ (second row in Table I), the W-dependence is seen to agree moderately well. For the nucleon terms alone Eq.(2) gives somewhat better results (Table I), but we don't expect this to hold for higher momentum transfers ($k^2 << -1(GeV/c)^2$).

There are precise experiments[7] measuring the total electroproduction cross section as a function of W. Because of the substantial nonresonant background which is indicated in a fit to the data we hesitate at the moment to compare our results concerning the resonance shape with experiment.

b) Magnetic Dipole, k^2-dependence

The k^2-dependence of $M_{1+}(W,k^2)$ is of course more sensitive to assumptions on the pion form factor than the resonance shape. If we neglect the variation of the latter, our ratio $R(W,k^2)$ of Eq.(19) agrees up to a normalization constant with the magnetic dipole transition form factor $G_M^*(k^2)$ defined by Ash et al.:[16]

$$\frac{G_M^*(k^2)}{G_M^*(0)} = R(W_r,k^2)\,\frac{G_M^p(k^2)}{G_M^p(0)} \quad . \tag{24}$$

In Fig.9 we compare this form factor with results obtained from an analysis of single arm electroproduction experiments[7] under

a) the assumptions (20) and

b) the assumption $F_\pi(k^2) = \dfrac{1}{1 - k^2/m_\rho^2}$. (25)

Clearly the second assumption fits the data better, but before one can take this as an indication for $F_\pi(k^2)$, the corresponding predictions for the smaller multipoles should be checked experimentally, since these depend stronger on $F_\pi(k^2)$.

c) Small Multipoles

In constrast to the magnetic dipole the amplitudes $E_{1+}(W,k^2)$ and $S_{1+}(W,k^2)$ obtain comparable contributions both from pion and nucleon exchange graphs, and these tend to cancel in $E_{1+}(W,k^2)$ near the resonance position, while in $S_{1+}(W,k^2)$ this occurs at threshold. Thus for assumption (20) $E_{1+}(W,k^2)$ is so small around $W = W_r$ that it will be hard to detect the sign. The scalar amplitude is a better candidate to check the model.

In Figs.10 and 11 we summarize the predictions for $E_{1+}(W,k^2)$ and $S_{1+}(W,k^2)$ by plotting the ratios

$$R_E(W,k^2) = \frac{|\vec{k}(W,0)|}{|\vec{k}(W,k^2)|} \frac{E_{1+}(W,k^2)}{M_{1+}(W,0)} \frac{G_M^p(0)}{G_M^p(k^2)} \tag{26}$$

and

$$R_S(W,k^2) = \frac{|\vec{k}(W,0)|}{|\vec{k}(W,k^2)|} \frac{S_{1+}(W,k^2)}{M_{1+}(W,0)} \frac{G_M^p(0)}{G_M^p(k^2)}$$

under assumption (20). The pion contributions alone are shown separately to allow for a modification due to a different pion form factor (as broken lines).

In connection with the scalar amplitude the question of gauge invariance should be mentioned. Clearly our model does not lead to a conserved current, since we do not couple the photon to all charged lines in our ladder diagrams. If we would include all those diagrams we would get ladder diagrams with a special class of vertex corrections as well as crossed box diagrams with attached ladders etc. Since we have included phenomenological vertex corrections anyhow and since we hope that non ladder diagrams play a minor role for our problem, we do not feel it urgent to include just those diagrams which restore gauge invariance. We hope that these diagrams are small corrections in the special gauge in which we are doing our calculation. This gauge is defined by the requirement that the virtual photon has no longitudinal component in the CMS (see Appendix A). It should be preferred to a gauge with vanishing scalar photons, because current conservation imposes zeros in W or k^2 on the longitudinal multipole, which require cancellations between various diagrams:
We have from current conservation

$$L_{1+}(W,k^2) = \frac{k_o}{|\vec{k}|} S_{1+}(W,k^2) \tag{27}$$

with

$$k_o = \frac{W^2 - M^2 + k^2}{2W} \quad ,$$

which may vanish in the physical region of electroproduction in contrast to $|\vec{k}|$. Thus the gauge invariance restoring diagrams possibly give relatively large corrections to L_{1+} in that region.

V. Comparison with other Models

There is a large number of dispersion theory models on the same subject, in which no adjustable parameters are needed. It is instructive to see how they differ from our approach, especially what kind of assumptions are made on the unphysical (left hand cut) singularities of the multipole amplitudes in these models. In our model the far away singularities are determined by both the Born terms and the iterations of the potential.

a) Born Approximation Model [4,5,17,18,19]

In this approach one assumes that the k^2- and the W-dependence of the amplitudes are determined by the on-shell transition potential:

$$M(W,k^2) \simeq \frac{M^{Born}(W,k^2)}{M^{Born}(W,0)} \; M(W,0) \quad . \tag{28}$$

The nearby left hand singularities of $M(W,k^2)$ which are those of $M^{Born}(W,k^2)$, are in general not well reproduced by Eq.(28), since the position of these singularities depends on k^2 , and in general $M(W,0)/M^{Born}(W,0) \neq 1$ at the singular points of $M(W,k^2)$. It is interesting to see whether an approximation like Eq.(28) can be gained from the Fredholm expansion[19] of the BSE.* Writing Eq.(2) in operator form as

$$M = M^{Born} + g^2 \, KM \; , \tag{29}$$

*This has been suggested in Ref.(18)

the Fredholm solution is[19]

$$M = M^{Born} + g^2 \, R \, M^{Born} \tag{30}$$

$$\text{with } R = \frac{K + \ldots}{1 - g^2 \, \mathrm{tr}\, K + \ldots} \quad . \tag{31}$$

Working with the lowest nontrivial approximation for R we get

$$M = \frac{M^{Born}(1 - g^2 \, \mathrm{tr}\, K) + g^2 \, K \, M^{Born}}{1 - g^2 \, \mathrm{tr}\, K} \quad . \tag{32}$$

It is not consistent to neglect the terms proportional to g^2 in the numerator, since at resonance, if our expansion is sufficiently good,

$$\mathrm{Re}(1 - g^2 \, \mathrm{tr}\, K) \approx 0$$

so that the k^2-dependence is given alone by the real part of the last term in the numerator of Eq.(32), which is the real part of the box diagram (the imaginary parts of the numerator cancel).

Another argument to justify Eq.(28) has been given by Walecka and Zucker.[5] They start from the full Omnès-solution of the partial wave dispersion relation, Eq.(12a), and approximate $M_L(W,k^2)$ by $M^{Born}(W,k^2)$ and propose that it is possible to take $M^{Born}(W',k^2)$ outside the dispersion integral:

$$\frac{1}{\pi} \int_{M+\mu}^{\infty} dW' \, \frac{\mathrm{Im}\, D(W') \, M^{Born}(W',k^2)}{W' - W - i\varepsilon} \approx \tag{33}$$

$$\approx \frac{M^{Born}(W,k^2)}{\pi} \int_{M+\mu}^{\infty} dW' \, \frac{\mathrm{Im}\, D(W')}{W' - W - i\varepsilon}$$

for $W \approx W_r$.

There are two difficulties in this procedure: First, if one evaluates Eq.(12a) with $M_L(W,k^2) = M^{Born}(W,k^2)$ numerically, assuming a reasonable phase shift, one does not obtain a result which shows much similarity with a resonant amplitude.[13] Either one has to add homogeneous solutions to (12a), or take a more refined function $M_L(W,k^2)$ as is done in this paper. Secondly, since $M^{Born}(W,k^2)$ is not constant with respect to W, taking it outside a principal value integral may introduce a very large error. Generally a principal value integral is very sensitive to the derivative of the integrand.

Concluding we think that Eq.(28) is an approximation which may be dangerous in quantitative applications. It leads to a stronger decrease with k^2 than Eq.(32), where the k^2-dependence is given by the off-shell Born term folded with the interaction potential. It also leads to an overestimate for the contribution of long range potentials if applied to the photoproduction amplitudes, where it reads

$$M(W,0) \simeq \frac{M^{Born}(W,0)}{f_{1+}^{Born}(W)} \; f_{1+}(W) \tag{34}$$

($f_{1+}(W)$ is the elastic scattering amplitude, $f_{1+}^{Born}(W)$ the scattering potential). Both these features are observed to be present in a comparison with experiment for $N^*(1236)$ production:[5] The predicted cross section decreases too rapidly with k^2, and the E_{1+}-amplitude is overestimated.

b) Nearby Singularity Model

Following the ideas of Chew, Goldberger, Low and Nambu,[20] Adler[2] proposed to start from Eq.(12a), but to use only the nearby singularities of $M_L(W,k^2)$, which of course are those of the Born terms $M^{Born}(W,k^2)$. To demonstrate the technique let us assume that we can approximate*

*In the following discussion we take amplitudes $M(W,k^2)$ where the threshold behavior has been devided out.

$$M_L(W,k^2) \approx M^{Born}(W,k^2) \approx \frac{C_1(k^2)}{W - W_1} \tag{35}$$

for not too high values of W. Then we easily get from Eq.(12b)

$$M(W,k^2) \approx \frac{D(W_1)}{D(W)} \frac{C_1(k^2)}{W - W_1} \quad . \tag{36}$$

But for this to be a good approximation we have to assume that there are no other poles or cuts in $M_L(W,k^2)$, which have residues comparable to $C_1(k^2)$ but which lie so far away that they do not disturb Eq.(35). Assume for instance

$$M_L(W,k^2) = \frac{C_1(k^2)}{W - W_1} + \frac{C_2(k^2)}{W - W_2} \tag{37}$$

with $C_2(k^2) \approx C_1(k^2)$

and $|W_2| >> |W_1|$,

so that Eq.(35) is still satisfied.

Then

$$M(W,k^2) = \frac{1}{D(W)} \left\{ C_1(k^2) \frac{D(W_1)}{W - W_1} + C_2(k^2) \frac{D(W_2)}{W - W_2} \right\} \quad . \tag{38}$$

But in the narrow resonance approximation we get,[2] if $\delta(\infty) = \pi$,

$$D(W) \approx \text{const } (W - W_r) \ , \tag{39}$$

so that the second term contributes as much as the first one.* Consequently it is not sufficient to show that $M_L(W,k^2)$ is reasonably well approximated by the nearby singularities of $M^{Born}(W,k^2)$. To get unique results one must have arguments or models specifying the residues of the far away singularities.

Once one has decided to forget distant singularities completely, this approach also explains the smallness of the E_{1+}-amplitude by the observation that the pion contributions are well represented by[2]

$$E^{Born}_{1+,\pi}(W,0) \approx \frac{C_3}{(W - W_3)^2} \qquad (40)$$

$$W_3 \approx M$$

from which one easily gets (considering Eq.(39))

$$E_{1+,\pi} \approx \frac{\text{const}}{D(W)} \frac{W_r - W}{(W - W_3)^2} \qquad (41)$$

which indeed vanishes at the resonance position.

c) Variational Techniques[3,22]

It is possible to find approximate solutions to the partial wave dispersion relation

$$\text{Re } M(W,k^2) = M_L(W,k^2) + \frac{P}{\pi} \int_{M+\mu}^{\infty} dW' \frac{\text{Im } M(W',k^2)}{W' - W} \quad , \qquad (42)$$

*These remarks are in very close analogy to the ideas proposed in Ref.(11), namely that it is possible to add homogenous contributions (Eq.(13)) to any solution as long as the asymptotic behavior of is not specified. Our discussion however is not restricted to the case $\delta(\infty) = \pi$.

subject to the final state interaction condition

$$M(W,k^2) = e^{i\delta} \, |M(W,k^2)| \ , \tag{43}$$

by making a suitable ansatz for $M(W,k^2)$ with variational parameters, which are determined by making the right and left hand sides of Eq.(42) to coincide as close as possible over the low energy region in W ($W \leq W_{max}$). This means one has a function satisfying

$$\text{Re } M(W,k^2) = M'_L(W,k^2) + \frac{P}{\pi} \int_{M+\mu}^{\infty} dW' \, \frac{\text{Im } M(W',k^2)}{W' - W} \tag{44}$$

$$\text{with } |M'_L(W,k^2) - M_L(W,k^2)| \ll |M_L(W,k^2)| \ , \tag{45}$$

$$W \leq W_{max} \ .$$

Now we have seen above that it is easy to construct functions which satisfy Eqs.(42) and (43), but whose inhomogeneous part $M''_L(W,k^2)$ is arbitrarily small compared to the complete real part, just by taking a single but distant pole for $M''_L(W,k^2)$. These functions may always be added to a solution of (42) without disturbing (45). Thus again one has to postulate the absence of far away singularities.
The results obtained in Ref.(3) are not very different from ours in the low k^2-region. We expect larger discrepancies to occur for $k^2 < -2(\text{GeV/c})^2$.

d) Zagury's Method.[1]

Zagury again starts from Eq.(12a) with

$$M_L(W,k^2) = M^{\text{Born}}(W,k^2) \ ,$$

but he does not take the expression (12c) for Im $D(W)$ but uses[22]

$$\text{Im } D(W) = -\rho(W)N(W)$$

where the kinematical factor $\rho(W)$ behaves like $O(W^3)$, $W \to \infty$. $N(W)$ is defined by

$$f_{1+}(W) = \frac{N(W)}{D(W)} \quad .$$

By approximating $N(W)$ by a single pole,

$$N(W) \approx \frac{\text{const}}{W - M}$$

the integral of Eq.(12a) becomes divergent. Zagury now uses the same method for the elastic scattering amplitude and assumes that the ratio of the amplitudes,

$$\frac{M(W,k^2)}{f_{1+}(W)}$$

can be approximated by the ratio of those two diverging integrals. This procedure has the advantage that the contributions to the integral (12a) for $M(W,k^2)$ come from high values of W . This might give similar effects as folding the off-shell Born terms with the wave function of the N^* .

e) Finally we want to compare the present calculations with a previous version,[23] where only the box diagrams had been used(besides the one particle exchange diagrams) to approximate the left hand cut. The box diagrams without cut-off actually are sufficient to give a reasonable left hand cut for the magnetic dipole in photoproduction, but the nucleon terms produced an E_{1+}-amplitude too high by a factor of two at least. Due to the introduction of cut-offs this term has almost disappeared. Also as a consequence of suppressing the high momentum components the form factors decrease faster with k^2 . This holds especially for the pion terms, and the quantitative difference may be seen from Fig.9 where the Curve c) corresponds to the results of Ref.(23) with $F_\pi(k^2) = G_E^p(k^2)$, and it should be compared to the Curve a).

VI. Conclusions

The present model uses phenomenological parameters, namely the three cut-off paramters Λ^2, Λ_N^2 and Λ_π^2 which determine the N^* scattering potential and the electromagnetic transition potential at short distances. It is our hope that our results for the energy and momentum transfer dependence of the multipoles do not depend too critically on the details of this short range modifications of the potentials, at least for moderate k^2. A better understanding of these parameters however is needed to justify their assumed k^2-independence.

We have emphasized the fact that, in conventional scattering theory language, the resonance pole contribution interferes in all resonant multipoles strongly with a nonresonant background which changes its shape with varying momentum tansfer, thus shifting the resonance peak to higher masses (if the threshold factor has been split off). Since in our model the background is generated by the same potential as the coupling to the resonance, the absence of such an effect would disproof the model. The present experimental situation is unclear because of the large nonresonant background in other partial waves, which maskes this effect. A detailed comparison with data will be given if experiments underway presently are finished.

If the indication taken from Fig.9 is correct that the pion form factor obeys ρ-dominance, then it should not be too difficult to isolate the contribution of the scalar amplitude S_{1+}, since it will be about 15% of M_{1+} at $k^2 = 1(\mathrm{GeV/c})^2$. The electric quadrupole E_{1+} however remains as difficult to find as it is in photoproduction.

Acknowlegement

The author appreciates many stimulating questions asked by Dr. W. Bartel and Dr. J. McElroy. He is deeply indebted to all the members of the DESY-Rechenzentrum for their continuous and effective help in programming difficulties.

References

1. N. Zagury, Phys. Rev. 145, 1112 (1966), ibid. 150, 1406 (1966)

2. S. L. Adler, Ann. Phys. (N.Y.) 50, 189 (1968)

3. G. v. Gehlen, Preprint (Weizmann Institute, 1969)

4. F. Selleri, V. Grecchi and G. Turchetti, Nuovo Cim. 52A, 314 (1967)

5. J. D. Walecka and P. A. Zucker, Phys. Rev. 167, 1479 (1968)
P. L. Pritchett, J. D. Walecka and P. A. Zucker, Preprint ITP-328 (Stanford 1969)

6. F. W. Brasse, J. Engler, E. Ganssauge and M. Schweizer, Nuovo Cim. 55A, 679 (1968)
H. L. Lynch, J. V. Allaby and D. M. Ritson, Phys. Rev. 164, 1635 (1967)
D. C. Imrie, C. Mistretta and R. Wilson, Phys. Rev. Letters 20, 1074 (1968)
W. Albrecht, F. W. Brasse, H. Dorner, W. Flauger, K. Frank, J. Gayler, H. Hultschig and J. May, DESY Report 68/48

7. W. Bartel, B. Dudelzak, H. Krehbiel, J. McElroy, V. Meyer-Berghout, W. Schmidt, V. Walther and G. Weber, Physics Letters 28 B 148, (1968)

8. F. Gutbrod, Nuovo Cim. 59 A, 293 (1969)

9. N. I. Muskhelishvili, Singular Integral Equations, Noordhoff, Groningen, 1953
R. Omnès, Nuovo Cim. 8, 316 (1954)

10. G. A. Baker, Advances in Theoretical Physics 1, 1 (1965) (Academic Press, New York)

11. D. Schwela, H. Rollnik, R. Weizel and W. Korth, Zeits. Phys. 202, 452 (1967)

12. Numerical values of the phase shifts are published by A. Domachie in Particle Interactions at High Energies (edited by T. W. Preist and L. L. J. Vick), Oliver and Boyd Edinburgh and London (1967)

13. K. D. Rothe, Phys. Rev. 170, 1548 (1968)

14. D. Schwela and R. Weizel, Z. Physik 221, 71 (1969)
D. Schwela, Thesis (Bonn 1968, unpublished)

15. H. P. Dürr and H. Pilkuhn, Nuovo Cim. 40, 899 (1965)

16. W. W. Ash, K. Berkelman, C. A. Lichtenstein, A. Romananskas and R. H. Siemann, Physics Letters 24, 165 (1967)

17. J. Benecke and H. P. Dürr, Nuovo Cim. 56, 267 (1968)

18. P. Dennery, Phys. Rev. 124, 2000 (1960)

19. S. L. Adler, Proceedings of the International Conference on Weak Interactions, Argonne National Laboratory Report AN L-7130, 285 (1965)

20. R. Courant and D. Hilbert, Methoden der Mathematischen Physik, Springer, Berlin (1968), I, p.121

21. G. F. Chew, M. L. Goldberger, F. Low and Y. Nambu, Phys. Rev. 106, 1345 (1957)

22. F. A. Behrends, A. Domachie and B. L. Weaver, Nucl. Phys. B 4, 1 (1968) ; ibid. B 4, 54 (1968)

23. G. F. Chew, S-Matrix Theory of Strong Interactions, Benjamin, New York (1961), P. 49

24. F. Gutbrod and D. Simon, Nuovo Cim. 51 A, 602 (1967)

25. M. L. Goldberger and K. M. Watson, Collision Theory, John Wiley and Sons, Inc., (New York), p. 202.

APPENDIX A: Off-Shell Electroproduction Bornterms

a) Nucleon Exchange Terms

The pion electroproduction matrix element according to the diagram of Fig.2a) is given by (omitting isospin variables)

$$\langle \pi\, N'e' | T | Ne \rangle = \varepsilon_\mu(k^2)\ \langle \pi N' | J^\mu | N \rangle \quad , \tag{A1}$$

$$\langle \pi N' | J_\mu | N \rangle = N\, \bar{u}\,(p_{N'}) \int d^4q\ T(p_{N'},q) \times$$

$$\times \frac{\not q - \frac{\not P}{2} + M}{\left((q+\frac{P}{2})^2 - \mu^2\right)\left((q-\frac{P}{2})^2 - M^2\right)}\ \Gamma_\mu(k,q)\ . \tag{A2}$$

The notation means:*

$$N = -\frac{ge}{2(2\pi)^2} \quad ,$$

$T(p_N,q)$ is a 4 x 4 off-shell scattering matrix which is given by a sum of ladder diagrams.

$$\Gamma_\mu(k,q) = \left(F_1(k^2)\gamma_\mu - iF_2(k^2)\sigma_{\mu\nu}k^\nu\right) \frac{\not q - \frac{\not P}{2} - \not k + M}{(q-\frac{P}{2}-k)^2 - M^2}\ \gamma_5\ u(p_N) \tag{A3}$$

---

*The normalization N is choosen such that if the d^4q-integration, the matrix $T(p_{N'},q)$ and the propagators in front of $\Gamma_\mu(k,q)$ are dropped, the matrix element reduces to an on-shell nucleon exchange matrix element for photoproduction with a photoproduction with a photon described by a polarization vector .

$$F_1(0) = \begin{cases} 1 \text{ for a exchanged proton} \\ 0 \text{ for a exchanged neutron} \end{cases}$$

$$F_2(0) = \frac{1}{2M} \begin{cases} 1.793 \text{ for proton} \\ -1.913 \text{ for neutron} \end{cases} \qquad \text{(A3)}$$

$$\varepsilon_\mu(k^2) = \frac{ie}{(2\pi)^{3/2}} \frac{1}{k^2} \bar{u}(e') \gamma_\mu u(e)$$

$$\frac{g^2}{4\pi} = 14.5$$

$$\frac{e^2}{4\pi} = \frac{1}{137}$$

P = total four momentum of πN-system.

With respect to gauge questions we shall proceed as follows:
The scalar component $J_o \equiv \langle \pi N' | J_o | N \rangle$ will be computed according to (A2) and the longitudinal component, defined originally by

$$J_\ell \equiv \frac{\vec{k}}{|\vec{k}|} \langle \pi N' | \vec{J} | N \rangle \qquad \text{(A4)}$$

will be taken to make the current conserved by brute force:

$$J_\ell = \frac{k_o}{|\vec{k}|} J_o \quad . \qquad \text{(A5)}$$

This result will in general not agree with that derived from (A4). It was discussed in Section 4 why we don't think this to be a serious defect. An equivalent procedure is to use[18]

$$\varepsilon'_\mu(k^2) = \varepsilon_\mu(k^2) - \frac{\varepsilon_\ell}{|\vec{k}|} k_\mu \qquad \text{(A6)}$$

with

$$\varepsilon_\ell = \vec{\varepsilon}(k^2) \cdot \frac{\vec{k}}{|\vec{k}|} = \varepsilon_o \frac{k_o}{|\vec{k}|}$$

instead of $\varepsilon_\mu(k^2)$ in (A;), i.e. to calculate in a gauge containing no longitudinal photons.
Now we write for $\not{q} - \frac{\not{P}}{2} + M$ in (A2) in the CMS ($\vec{p} = 0$)

$$\not{q} - \frac{\not{P}}{2} + M = \sum_{i = 1,2} \alpha_i \sum_{s=1,2} u_{s,i}(\vec{q})\ \bar{u}_{s,i}(\vec{q})$$

with

$$\alpha_i = \frac{1}{2}\left(1 + \frac{W - 2q_o}{r_i}\right)$$

and $u_{s,i}(q)$ being a Dirac spinor with spin index s and energy*
$r_i = \pm\sqrt{\vec{q}^2 + M^2}$ (+ for i = 1, - for i = 2). Therefore we are left with the task of performing a multipole analysis of the matrix element

$$M_{off} = \bar{u}_{s,i}(\vec{q})\ \Gamma_\mu(k,q)\ \varepsilon^\mu(k^2) \quad . \tag{A7}$$

The only difference to the usual projection technique is due to the fact that $\vec{q}$ is an off-shell three momentum, and

$$r_i + \frac{P_o}{2} + q_o \neq W \ .$$

At first we brak down the matrix element (A7) into a matrix element between Pauli spinors:

(A8)

$$M_{oo} = \frac{W}{\pi}\{ i\,\vec{\sigma}\,\vec{\varepsilon}'\,\mathcal{F}_1 + \vec{\sigma}\cdot\hat{q}\,\vec{\varepsilon}'\cdot(\vec{\sigma}\times\hat{k})\,\mathcal{F}_2 + i\,\vec{\sigma}\cdot\hat{k}\,\hat{q}\cdot\vec{\varepsilon}'\,\mathcal{F}_3 +$$

$$+ i\,\vec{\sigma}\cdot\hat{q}\,\hat{q}\cdot\vec{\varepsilon}'\,\mathcal{F}_4 - i\,\vec{\sigma}\cdot\hat{q}\,\varepsilon_o'\,\mathcal{F}_7 - i\,\vec{\sigma}\cdot\hat{k}\,\varepsilon_o'\,\mathcal{F}_8\} \ ,$$

---

*Negative energy spinors are defined by $u_{s,2}(\vec{q}) = \frac{1}{\sqrt{r_2+M}}(\not{r} + M)\begin{pmatrix}\chi_s\\ 0\end{pmatrix}$, $r = (r_2, \vec{q})$.
The square root always drops out in the following.

$$\hat{q} = \frac{\vec{q}}{|\vec{q}|} \quad ,$$

$$\hat{k} = \frac{\vec{k}}{|\vec{k}|} \quad .$$

We list those contributions to $\mathcal{F}_i$ separately which are proportional to $F_1(k^2)$ and $F_2(k^2)$ (we omit the coefficients $\mathcal{F}_5$ and $\mathcal{F}_6$, which we don't need):

$$\mathcal{F}_1 = - A \sqrt{(E_1 + M)(r_i + M)} \{W' - M\} \tag{A 9}$$

$$\mathcal{F}_2 = A \sqrt{(E_1 - M)(r_i - M)} \{W' + M\} \tag{A10}$$

$$\mathcal{F}_3 = -2 A \sqrt{(E_1 - M)(r_i - M)} \{r_i + M\} \tag{A11}$$

$$\mathcal{F}_4 = 2 A \sqrt{(E_1 + M)(r_i + M)} \{r_i - M\} \tag{A12}$$

$$\mathcal{F}_7 = - A \sqrt{(E_1 + M)(r_i - M)} \{r_i - \varepsilon_\pi + M\} \tag{A13}$$

$$\mathcal{F}_8 = A \sqrt{(E_1 - M)(r_i + M)} \{r_i - \varepsilon_\pi - M\} \tag{A14}$$

$$\text{with } A = - \frac{F_1(k^2)}{u - M^2} \frac{\pi N}{W}, \tag{A15}$$

$$u = (q - \frac{P}{2} - k)^2 ,$$

$$\varepsilon_\pi = q_o + \frac{W}{2} = \text{pion off-shell CM-energy} ,$$

$$W' = r_i + \varepsilon_\pi \quad .$$

The contributions proportional to $F_2(k^2)$ are:

$$\mathcal{F}_1 = B\sqrt{(E_l + M)(r_i + M)}\,\{u - M^2 + 2M(W' - M) + (W - W')(W' - M - 2\varepsilon_\pi)\} \tag{A16}$$

$$\mathcal{F}_2 = B\sqrt{(E_l - M)(r_i - M)}\,\{u - M^2 - 2M(W' + M) + (W - W')(W' + M - 2\varepsilon_\pi)\} \tag{A17}$$

$$\mathcal{F}_3 = 2B\sqrt{(E_l - M)(r_i - M)}\,\{r_i + M)(W + M)\} \tag{A18}$$

$$\mathcal{F}_4 = B\sqrt{(E_l + M)(r_i + M)}\,\{(r_i - M)(W - M)\} \tag{A19}$$

$$\mathcal{F}_7 = -B\sqrt{(E_l + M)(r_i - M)}\,\{u - M^2 + \vec{q}^2 - \varepsilon_\pi^2 + (E_l + M)\varepsilon_\pi + (E_l - M)(r_i + M)\} \tag{A20}$$

$$\mathcal{F}_8 = -B\sqrt{(E_l - M)(r_i + M)}\,\{u - M^2 + \vec{q}^2 - \varepsilon_\pi^2 + (E_l - M)\varepsilon_\pi + (E_l + M)(r_i - M)\} \tag{A21}$$

$$B = \frac{F_2(k^2)}{u - M^2}\,\frac{\pi N}{W} \quad . \tag{A22}$$

If we introduce a cut-off in the nucleon propagator as in Eq.(4), we simply have to redefine A and B:

$$A \Rightarrow A \cdot \frac{\Lambda_N^2}{\Lambda_N^2 + M^2 - u} \tag{A23}$$

and

$$B \Rightarrow B \cdot \frac{\Lambda_N^2}{\Lambda_N^2 + M^2 - u} \quad . \tag{A24}$$

Multipole projection is done by the formulas[22]

$$M_{\ell+} = \frac{1}{\ell+1}\ \frac{1}{2}\int_{-1}^{+1} dx\ \{P_\ell(x)\,\mathcal{F}_1 - P_{\ell+1}(x)\,\mathcal{F}_2 - \frac{1}{2\ell+1}\left(P_{\ell-1}(x) - P_{\ell+1}(x)\right)\mathcal{F}_3\}\ , \tag{A25}$$

$$E_{\ell+} = \frac{1}{\ell+1}\ \frac{1}{2}\int_{-1}^{+1} dx\ \{P_\ell(x)\,\mathcal{F}_1 - P_{\ell+1}\,\mathcal{F}_2 + \frac{1}{2\ell+1}\left[P_{\ell-1}(x) - P_{\ell+1}(x)\right]\mathcal{F}_3 + \frac{\ell+1}{2\ell+3}\left[P_\ell(x) - P_{\ell+2}(x)\right]\mathcal{F}_4\}\ , \tag{A26}$$

$$S_{\ell+} = \frac{1}{\ell+1}\ \frac{1}{2}\int_{-1}^{+1} dx\ \{P_{\ell+1}(x)\,\mathcal{F}_7 + P_\ell(x)\,\mathcal{F}_8\}\ , \tag{A27}$$

$$u = M^2 + \varepsilon_\pi^2 - \vec{q}^{\,2} - 2E_1\varepsilon_\pi - 2|\vec{k}|\ |\vec{q}|\ x\ .$$

We do not write down the resulting expressions for M_{l+} etc., which follows from (A8) - (A26). The modification due to the cut-off are analogous to Eq.(5) except for those terms in Eqs.(A15) -(A20) which are proportional to $u - M^2$. For instance the first term in Eq.(A16) contributes to M_{l+} as

$$-\sqrt{(E_l + M)(r_i + M)}\ \frac{F_2(k^2)\cdot\Lambda_N^2}{4\ |\vec{k}|\ |\vec{q}|}\ \frac{\pi N}{W}\ Q_l(Z') \tag{A28}$$

with

$$Z' = \{(E_l - \varepsilon_\pi)^2 - \vec{k}^{\,2} - \vec{q}^{\,2} - M^2 - \Lambda_N^2\}\ /2|\vec{q}|\,|\vec{k}| \tag{A29}$$

For $\ell > 0$ these terms of course vanish in the limit $\Lambda_N^2 \to \infty$.

b) Pion Exchange Terms

The pion diagram Fig.2b) is obtained from Eq.(A2) by setting

$$\Gamma_\mu(k,q) = \frac{F_\pi(k^2)}{(q + \frac{P}{2} - k)^2 - \mu^2} \; (2q + P - k)_\mu \; \gamma_5 \; u(p_N) \; . \tag{A30}$$

The contribution to the $\mathcal{F}_i$-amplitudes is given by

$$\mathcal{F}_1 = \mathcal{F}_2 = 0 \tag{A31}$$

$$\mathcal{F}_3 = 2 \; C \; \sqrt{(E_1 - M)(r_i + M)} \; |\vec{q}| \tag{A32}$$

$$\mathcal{F}_4 = -2C \; \sqrt{(E_1 + M)(r_i - M)} \; |\vec{q}| \tag{A33}$$

$$\mathcal{F}_7 = C \; \sqrt{(E_1 + M)(r_i - M)} \; \{2\varepsilon_\pi - k_o\} \tag{A34}$$

$$\mathcal{F}_8 = - C \; \sqrt{(E_1 - M)(r_i + M)} \; \{2\varepsilon_\pi - k_o\} \tag{A35}$$

$$C = \frac{F_\pi(k^2)}{(q + \frac{P}{2} - k)^2 - \mu^2} \; \frac{\pi N}{W} \; . \tag{A36}$$

With a cut-off in the pion propagator we get

$$C \Rightarrow \frac{C \; \Lambda_\pi^2}{\Lambda_\pi^2 + \mu^2 - (q + \frac{P}{2} - k^2)} \; . \tag{A37}$$

APPENDIX B: Connection Between the Range of the Transition Potential and the Resonance Shape of a Multipole

We want to give a simple consideration how the mismatch of a transition potential and a scattering potential can cause an unusual energy behavior of a resonant inelastic amplitude. Let us discuss the electrodisintegration of a bound state of zero angular momentum between a charged and neutral particle leading to a final resonating state between these particles. In nonrelativistic potential theory the transition amplitude $E(\varepsilon)$ is determined by the Lippman-Schwinger equation[24]

$$E(\varepsilon) = \langle \phi^{-}(\varepsilon) | V_\gamma | \phi_o \rangle$$

$$= E^{Born}(\varepsilon|\varepsilon) + \frac{1}{\pi} \int_0^\infty dk^2 \; \frac{f(\varepsilon|k^2) E^{Born}(k^2|\varepsilon)}{k^2 - \varepsilon - i0} \quad , \qquad (B1)$$

with the following notation:

ϕ_o = wave functions of initial bound state,

$\phi^{-}(\varepsilon)$ = wave functions of final scattering state of energy ε ,

$E^{Born}(k^2|\varepsilon) = \langle$ plane wave, $k|V_\gamma|\ \phi_o \rangle$

= off-shell matrix element of transition operator V_γ between bound state and plane wave of momentum k,

$f(\varepsilon|k^2)$ = off-shell scattering amplitude of the two particles at energy ε .

The scattering amplitude is assumed to satisfy the elastic Lippman-Schwinger equation

$$f(\varepsilon,\varepsilon) = f^{Born}(\varepsilon|\varepsilon) + \frac{1}{\pi} \int_o^\infty \frac{f(\varepsilon|k^2)\ f^{Born}(k^2|\varepsilon)}{k^2 - \varepsilon - i0} \qquad (B2)$$

and should have a broad resonance at $\varepsilon = \varepsilon_r$.
Assume now that

$$E^{Born}(\varepsilon|k^2) \approx \rho(k^2)\ f^{Born}(\varepsilon|k^2) \qquad \text{for} \quad \varepsilon \simeq \varepsilon_r \qquad (B3)$$

where $\rho(k^2)$ decreases with increasing k^2 , what will be the case if the charged particle is much lighter than the mass of the particle which is exchanged in the final state. The influence of such a function on the resonance shape is best seen from the imaginary part of $E(\varepsilon)$:

$$\mathrm{Im}\ E(\varepsilon) \approx E^{Born}(\varepsilon|\varepsilon)\ \mathrm{Re}\ f(\varepsilon|\varepsilon) + \frac{P}{\pi}\int_0^\infty dk^2\ \frac{\mathrm{Im}\ f(\varepsilon|k^2)\ f^{Born}(k^2|\varepsilon)\rho(k^2)}{k^2 - \varepsilon} \qquad (B4)$$

The first term in (B4) changes sign at $\varepsilon = \varepsilon_r$. The sign of the principal value integral depends on $\rho(k^2)$: If this function supresses the integrand in the region $k^2 > \varepsilon_r$, the contributions from $k^2 < \varepsilon_r$ will dominate and the integral also changes sign for sufficiently large ε , which may introduce a zero in $\mathrm{Im}E(\varepsilon)$ within the width Γ of the resonance, if this is sufficiently broad. As a qualitative condition for that to occur one expects that it is necessary for $\rho(k^2)$ to vary strongly in the region

$$\varepsilon_r - \frac{\Gamma}{2} < k^2 < \varepsilon_r + \frac{\Gamma}{2} \quad .$$

If the mass of the charged particle is comparable to the resonance width this is expected to hold. Note that for $\rho(k^2) = \mathrm{const}$ there can be no zero in $\mathrm{Im}\ E(\varepsilon)$ since $\mathrm{Im}\ f(\varepsilon|\varepsilon) \geq 0$.

$W[\mu]$	7.73	8.0	8.5	9.0	9.5	10.0
W[GeV]	1.079	1.117	1.186	1.256	1.326	1.396
$R_{N+\pi}^{Born}(W,k^2)$	0.311	0.360	0.431	0.486	0.531	0.568
Same, but normalized.	0.469	0.542	0.649	0.732	0.799	0.856
$R(W,k^2)$	0.417	0.494	0.619	0.732	0.845	0.973
$R_N^{Born}(W,k^2)$	0.511	0.556	0.608	0.641	0.665	0.684
Same, but normalized.	0.625	0.680	0.744	0.785	0.814	0.837
$R_N(W,k^2)$	0.597	0.652	0.726	0.785	0.843	0.909

TABLE I Ratios between Born terms of $M_{1+}(W,k^2)$ for $k^2 = -1\ (GeV/c)^2$ and $k^2 = 0$.
The second and fifth row are the same ratios normalized to those of the Bethe-Salpeter amplitudes at $W = q\mu$. $R_{N+\pi}^{Born}(W,k^2)$ is defined in Eq.(22), $R_N^{Born}(W,k^2)$ in Eq.(23) and $R(W,k^2)$ in Eq.(19). $R_N(W,k^2)$ is defined analogously to $R(W,k^2)$ with only the nucleon exchange contributions.

Figure Captions

Fig.1 a) Nucleon exchange contribution to $\gamma N \to \pi N$ transition potential.

b) Pion exchange contribution to $\gamma N \to \pi N$ transition potential.

Fig.2 a) Nucleon current contribution to the γNN^* vertex.

b) Pion current contribution to the γNN^* vertex.

Fig.3) Contour C_W in the complex W-plane, on which the Bethe-Salpeter equation has been iterated.

Fig.4) Graphical representation of the Bethe-Salpeter equation for N^*-electroproduction.

Fig.5) Ratio $|\vec{p}|E_{1+}(W,0)/|\vec{k}|f_{1+}(W)$ for different values of the cut-off parameter Λ_π^2 which are shown besides the curves.

Fig.6) Ratio $|\vec{p}|M_{1+}(W,0)/|\vec{k}|f_{1+}(W)$ for different values of the cut-off parameter Λ_N^2 with $\Lambda_\pi^2 = 0.5\ \mathrm{GeV}^2$. The data are taken from Ref.(14).

Fig.7) Argand-diagrams for $|\vec{p}|M_{1+}(W,0)$ and $|\vec{p}|E_{1+}(W,0)$. The numbers attached to the curves are the photon Lab.-momenta.

Fig.8) Ratio $|\vec{k}(W,0)|M_{1+}(W,k^2)/|\vec{k}(W,k^2)|M_{1+}(W,0)\,G_E^p(k^2)$ for different values of k^2. It was assumed that $F_\pi(k^2) = G_E^p(k^2)$.

Fig.9) Comparison of the γNN^* form factor $G_M^*(k^2)$ with experiment[7] under the assumptions (20) (Curve a) and (25) (Curve b). Curve c is taken from Ref.(23).

Fig.10 a) and b): The ratio $|\vec{k}(W,0)|E_{1+}(W,k^2)/|\vec{k}(W,k^2)|M_{1+}(W,0)\cdot G_E^p(k^2)$ for different values of k^2. (in$(GeV/c)^2$). The broken lines are the pion contributions alone.

Fig.11 a) and b): The ratio $|\vec{k}(W,0)|S_{1+}(W,k^2)/|\vec{k}(W,k^2)|M_{1+}(W,0)G_E^p(k^2)$ for different values of k^2 (in $(GeV/c)^2$). The broken lines are the pion contributions alone. The relation (20) has been assumed.

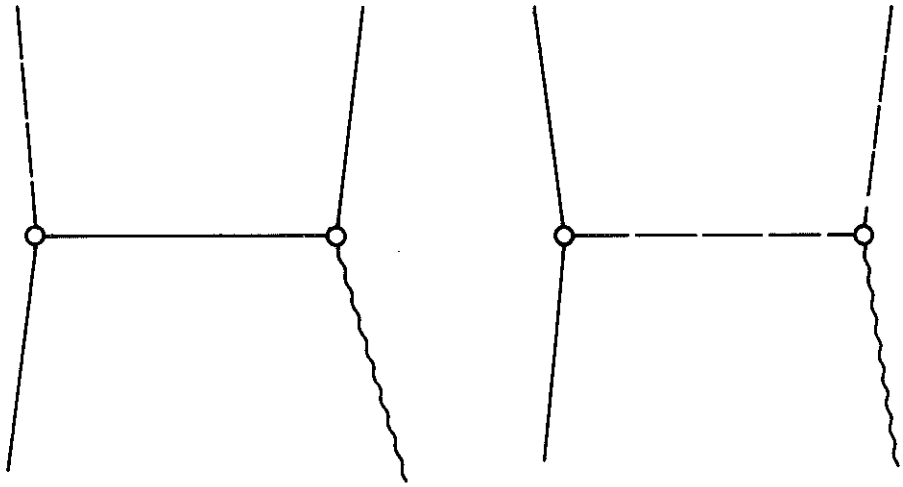

Fig. 1

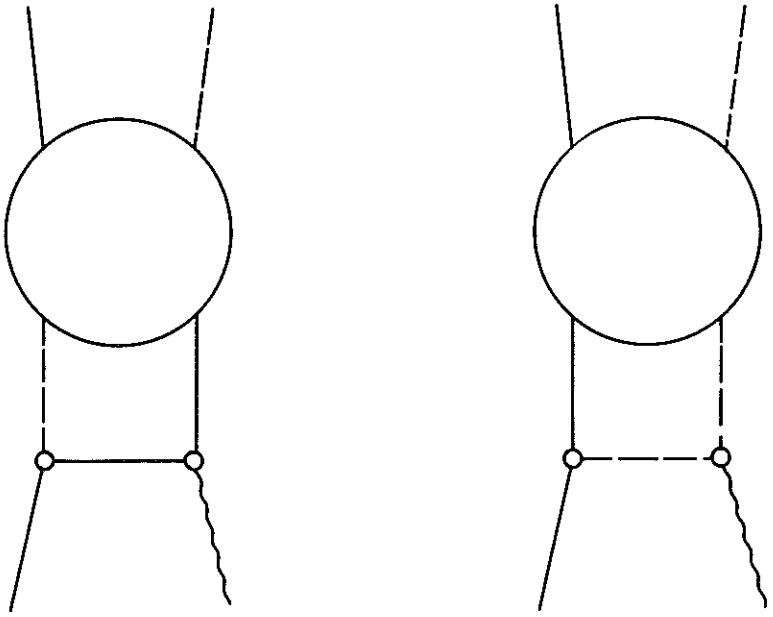

Fig. 2

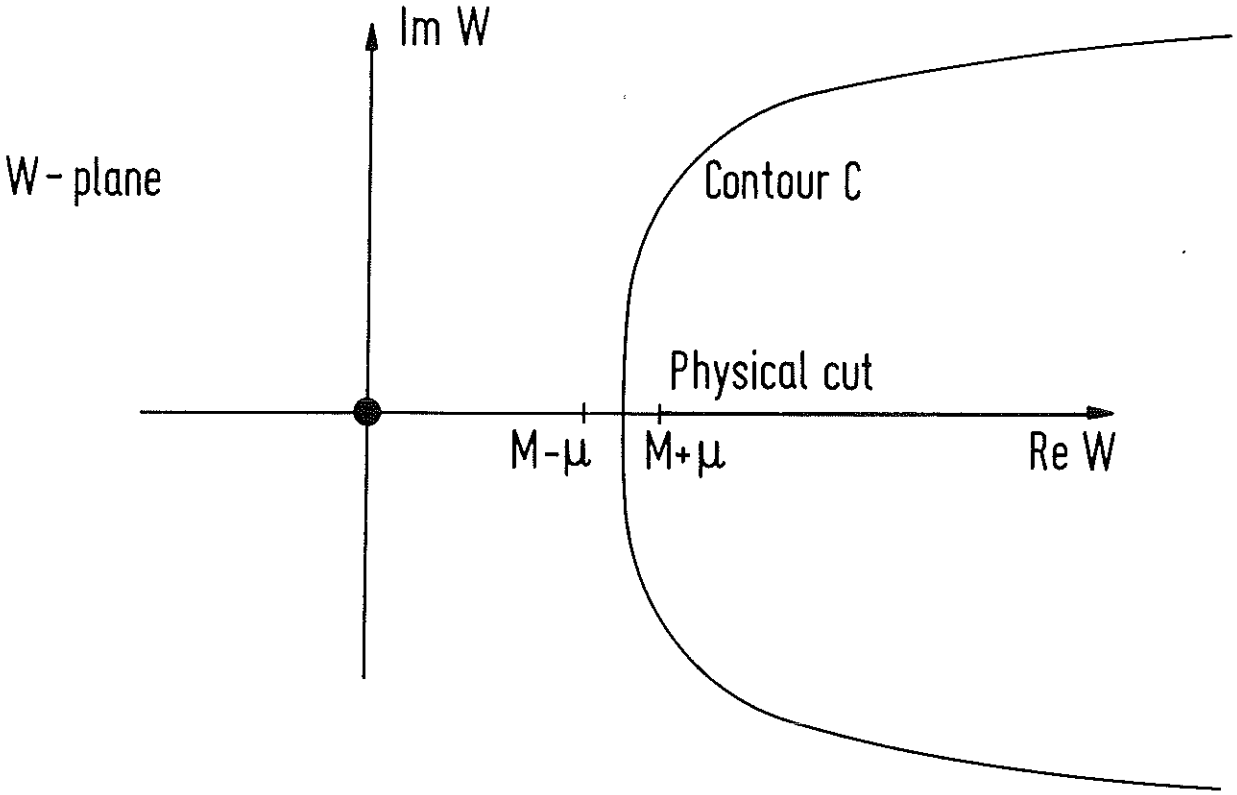

Fig. 3

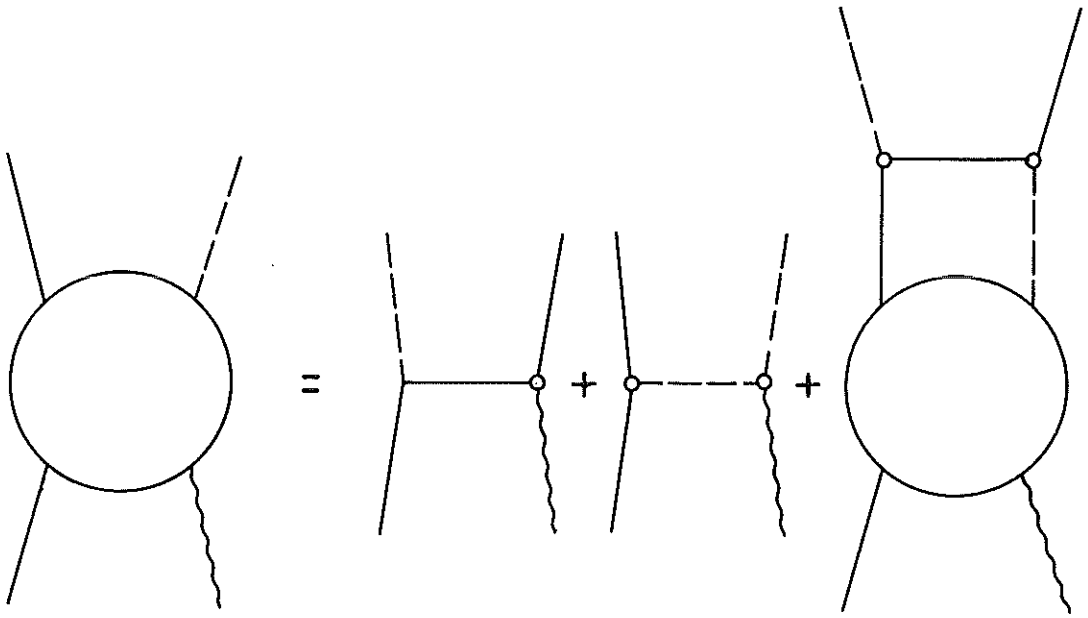

Fig. 4

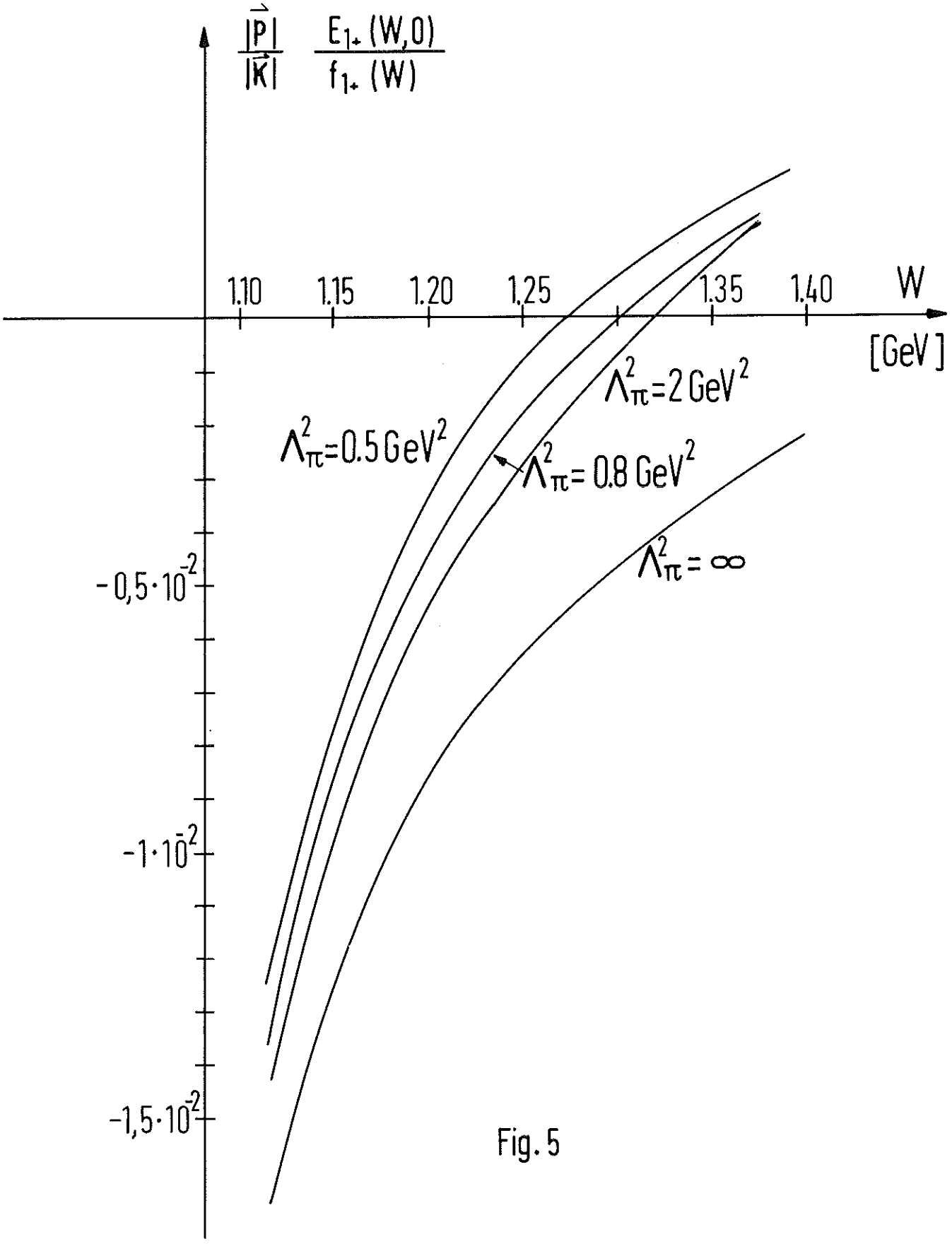
$\frac{|\vec{P}|}{|\vec{K}|}\ \frac{E_{1+}(W,0)}{f_{1+}(W)}$
1.10
1.15
1.20
1.25
1.35
1.40
W
[GeV]
$\Lambda^2_\pi = 2\,GeV^2$
$\Lambda^2_\pi = 0.5\,GeV^2$
$\Lambda^2_\pi = 0.8\,GeV^2$
$\Lambda^2_\pi = \infty$
$-0,5\cdot10^{-2}$
$-1\cdot10^{-2}$
$-1,5\cdot10^{-2}$

Fig. 5

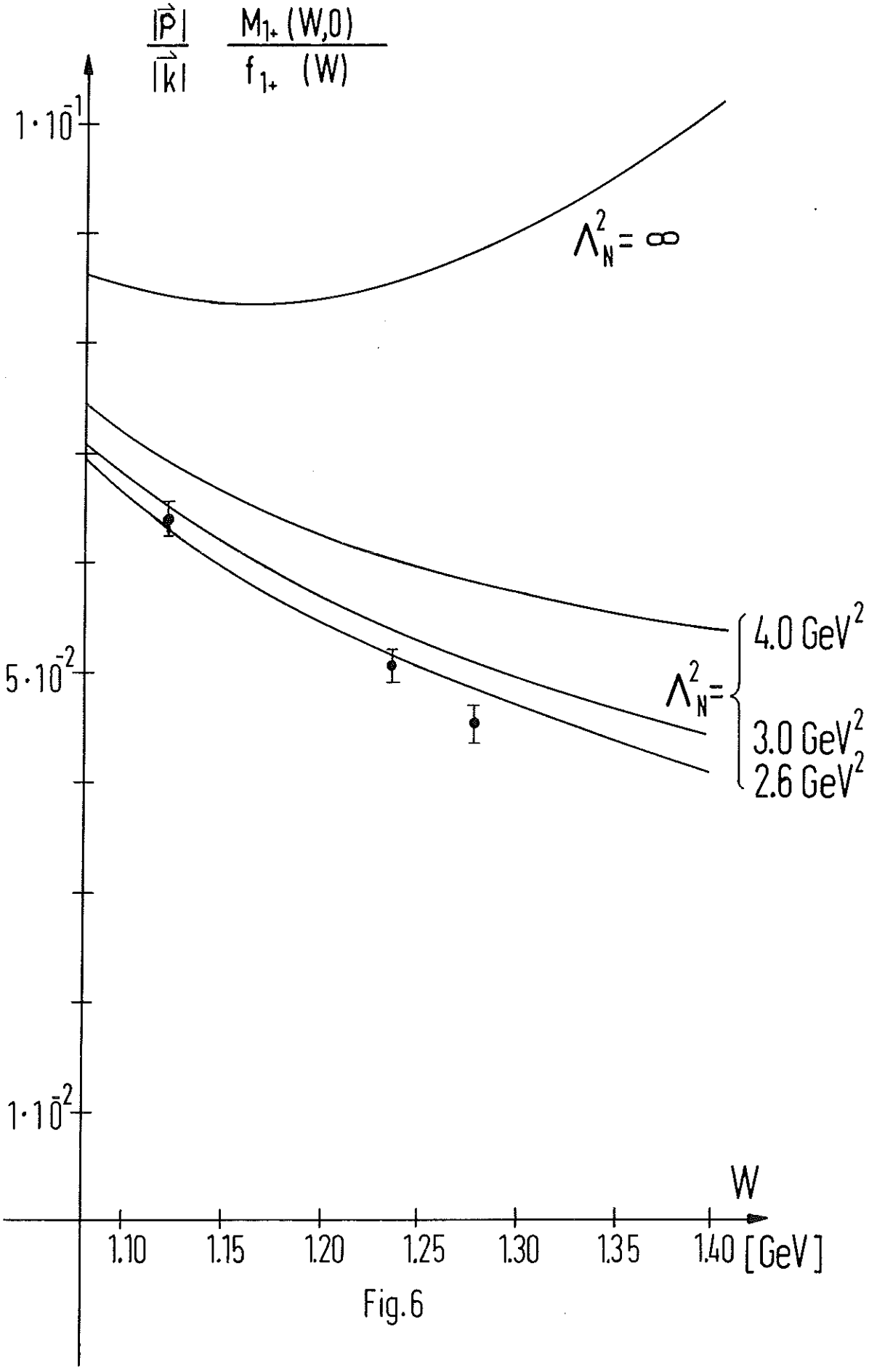
$\frac{|\vec{P}|}{|\vec{k}|} \quad \frac{M_{1+}(W,0)}{f_{1+}(W)}$
$1 \cdot 10^{-1}$
$5 \cdot 10^{-2}$
$1 \cdot 10^{-2}$
$\Lambda_N^2 = \infty$
$\Lambda_N^2 =$
4.0 GeV^2
3.0 GeV^2
2.6 GeV^2
W
1.10
1.15
1.20
1.25
1.30
1.35
1.40 [GeV]

Fig. 6

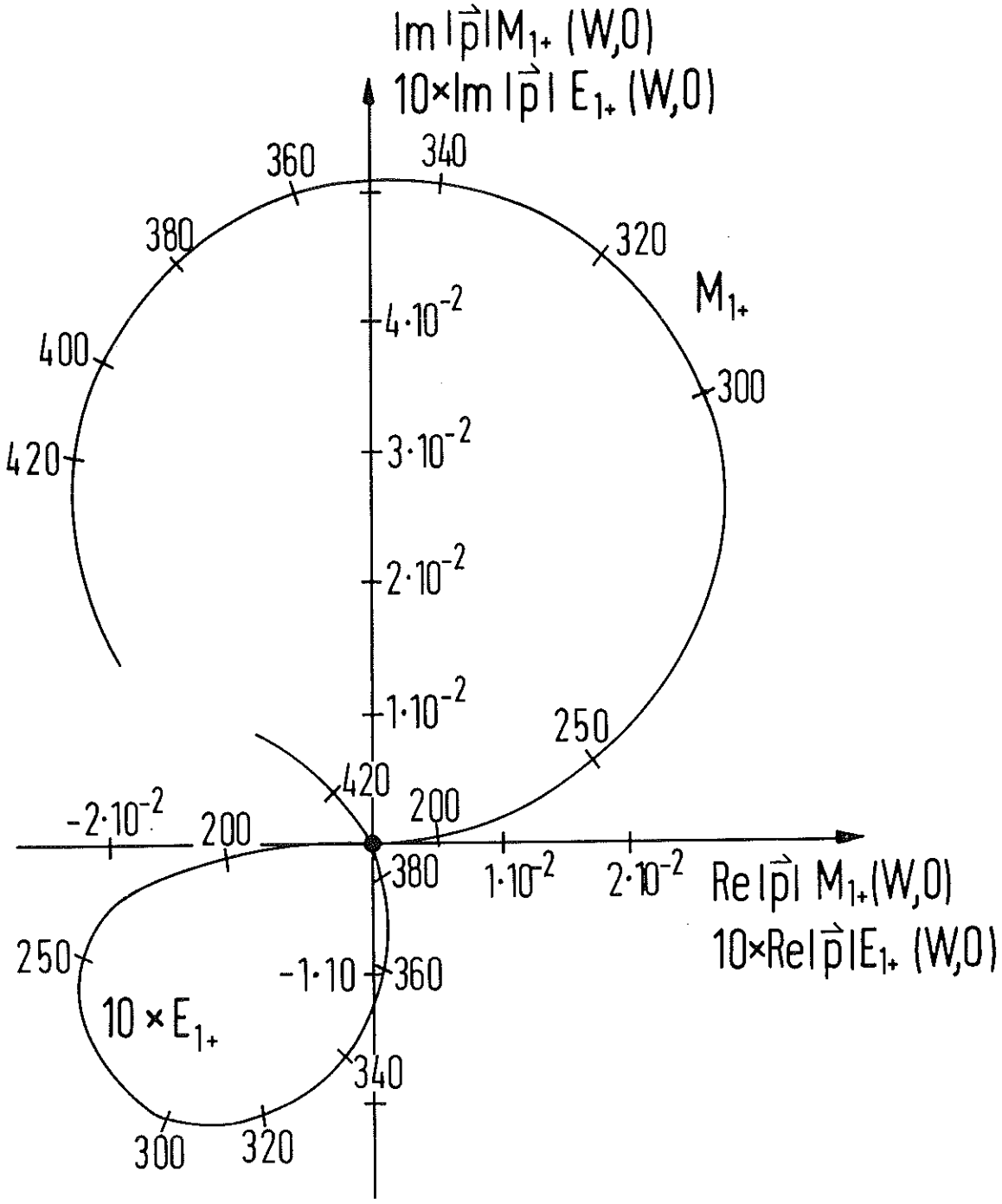
Im |p| M1+ (W,0)
10×Im |p| E1+ (W,0)
360
340
380
320
M1+
400
300
420
4·10-2
3·10-2
2·10-2
1·10-2
250
420
200
-2·10-2
200
380
1·10-2
2·10-2
Re |p| M1+(W,0)
10×Re |p| E1+ (W,0)
250
-1·10
360
10 × E1+
340
300
320

Fig. 7

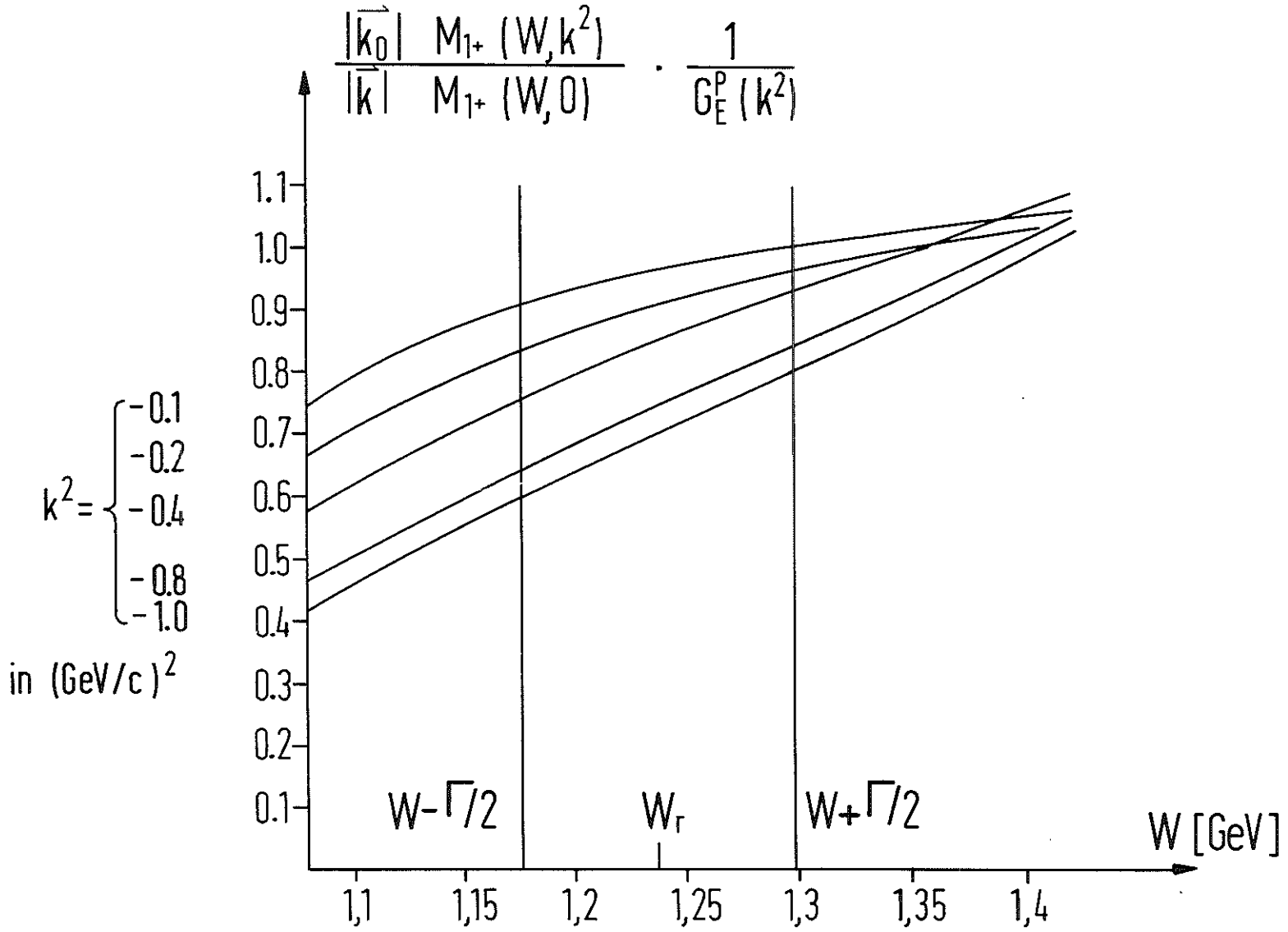
$\frac{|\vec{k_0}|\ M_{1+}(W,k^2)}{|\vec{k}|\ M_{1+}(W,0)} \cdot \frac{1}{G_E^p(k^2)}$
1.1
1.0
0.9
0.8
0.7
0.6
0.5
0.4
0.3
0.2
0.1
$k^2 =$ -0.1 -0.2 -0.4 -0.8 -1.0
in $(GeV/c)^2$
$W-\Gamma/2$
W_r
$W+\Gamma/2$
W [GeV]
1,1
1,15
1,2
1,25
1,3
1,35
1,4

Fig.8

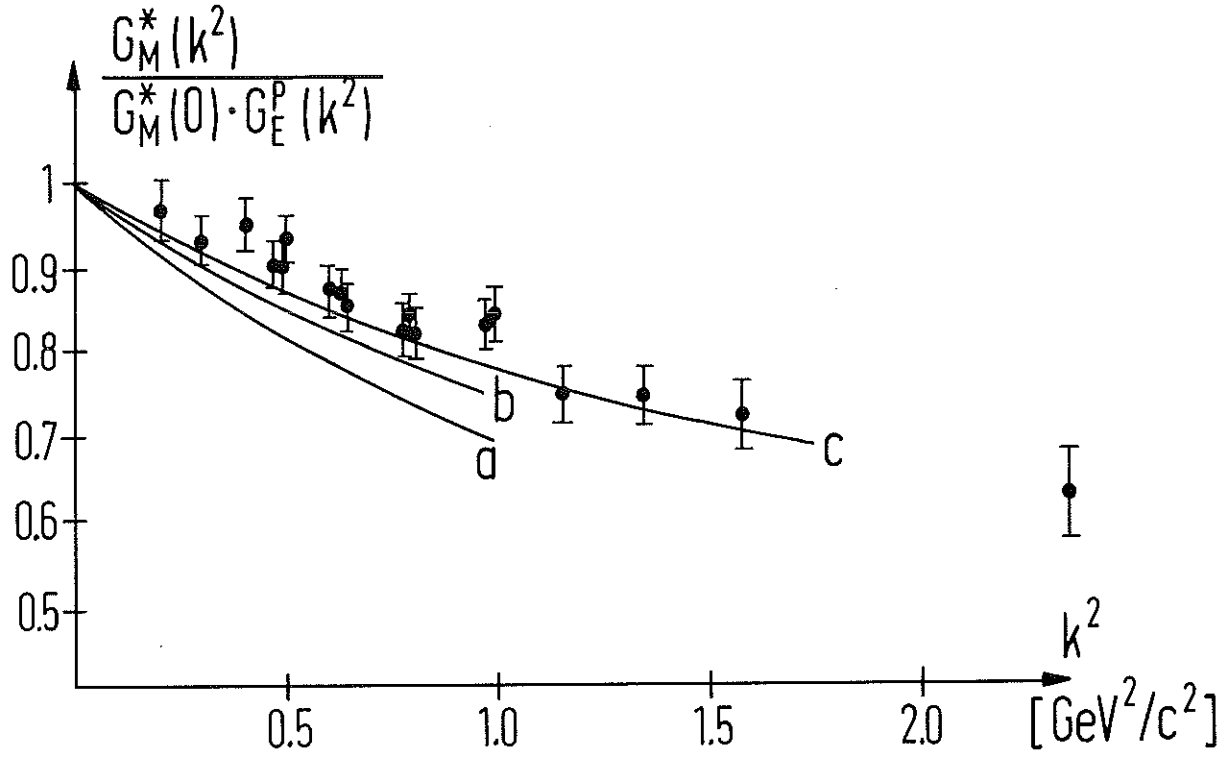
$\frac{G_M^*(k^2)}{G_M^*(0)\cdot G_E^p(k^2)}$
1
0.9
0.8
0.7
0.6
0.5
a
b
c
k^2
0.5
1.0
1.5
2.0
$[GeV^2/c^2]$

Fig. 9

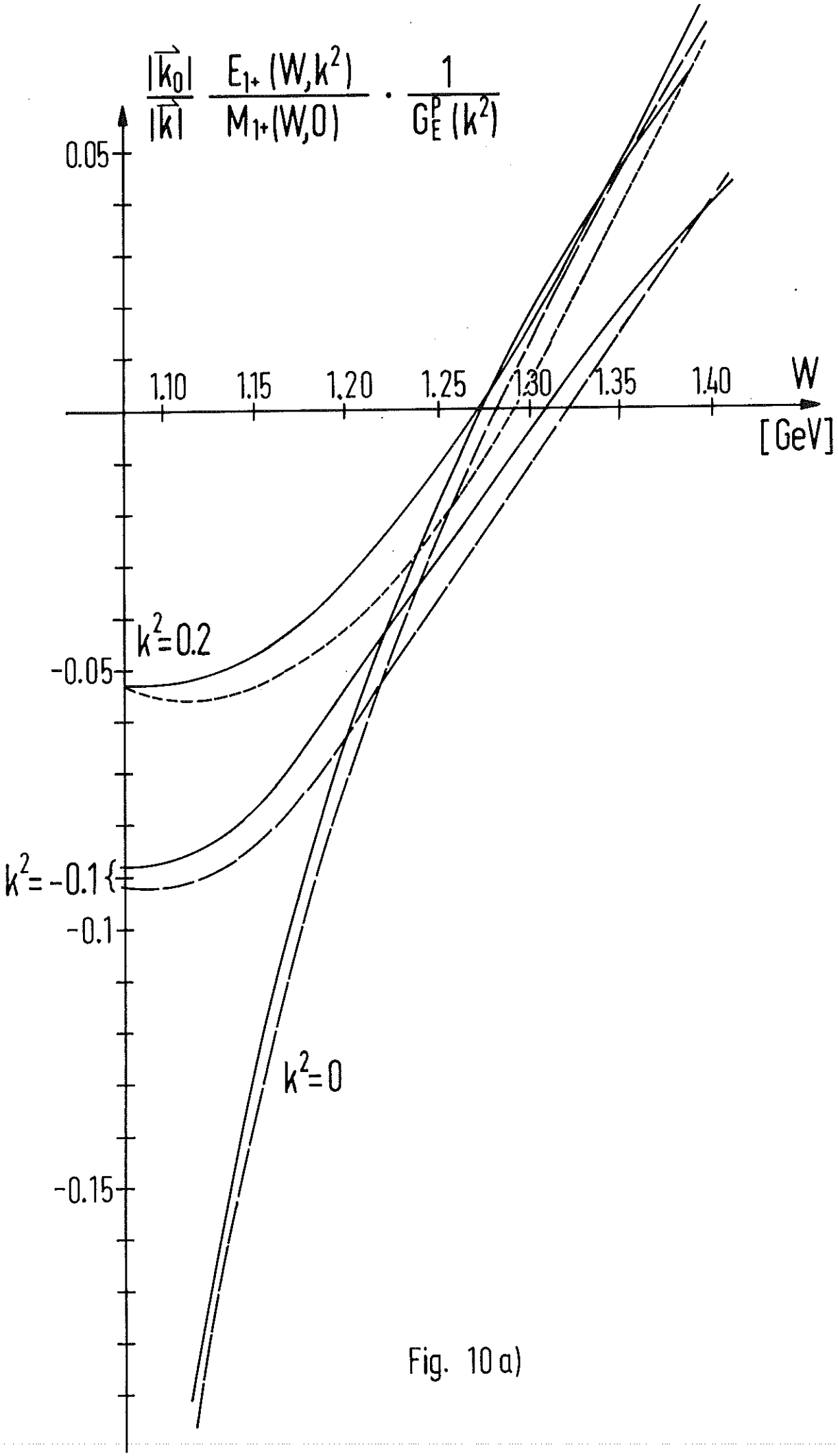
$\frac{|\vec{k}_0|}{|\vec{k}|} \frac{E_{1+}(W,k^2)}{M_{1+}(W,0)} \cdot \frac{1}{G_E^p(k^2)}$
0.05
-0.05
-0.1
-0.15
1.10
1.15
1.20
1.25
1.30
1.35
1.40
W
[GeV]
$k^2=0.2$
$k^2=-0.1$
$k^2=0$

Fig. 10 a)

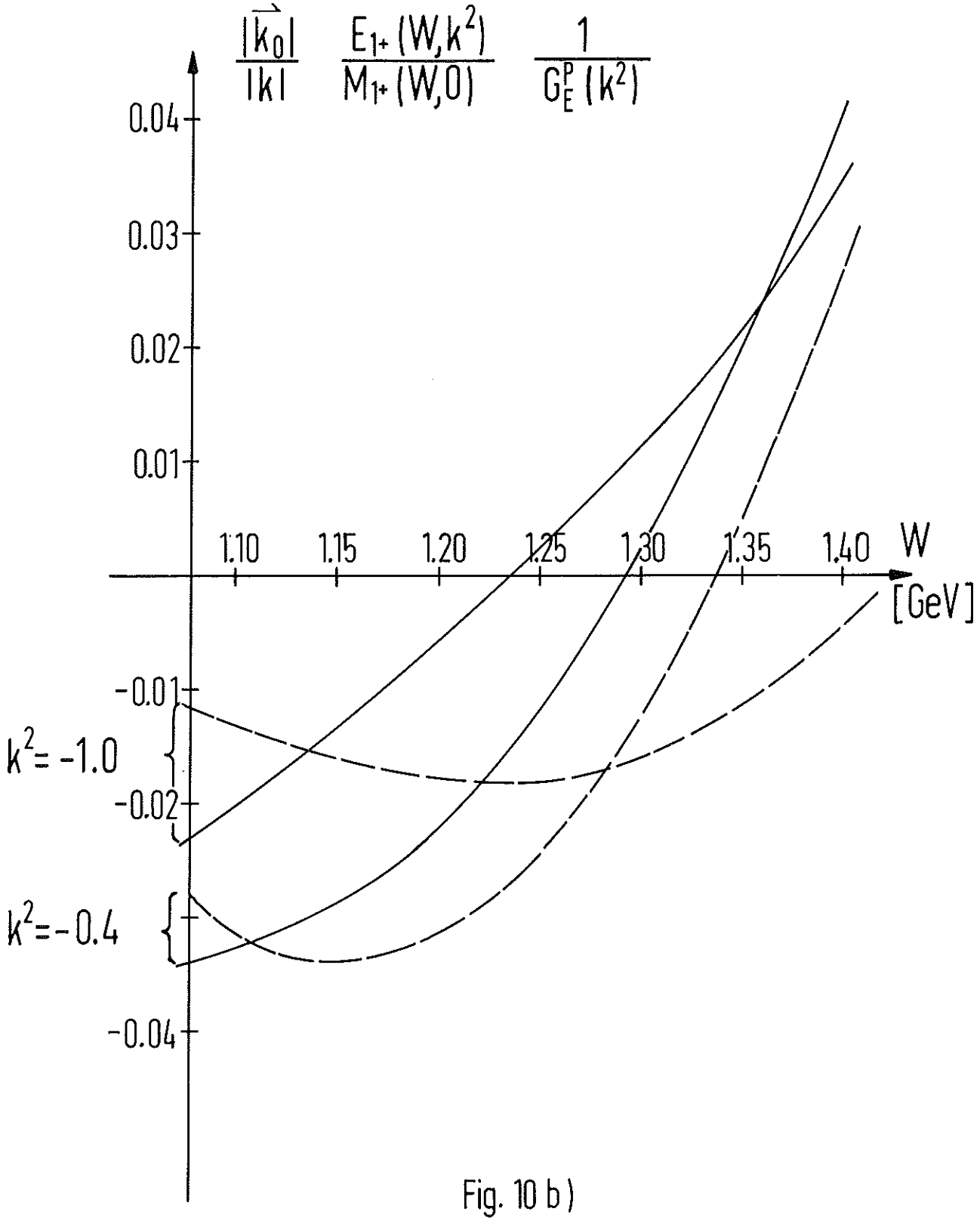
$\frac{|\vec{k}_0|}{|k|}$ $\frac{E_{1+}(W,k^2)}{M_{1+}(W,0)}$ $\frac{1}{G_E^p(k^2)}$
0.04
0.03
0.02
0.01
-0.01
-0.02
-0.04
1.10
1.15
1.20
1.25
1.30
1.35
1.40
W
[GeV]
$k^2 = -1.0$
$k^2 = -0.4$

Fig. 10 b)

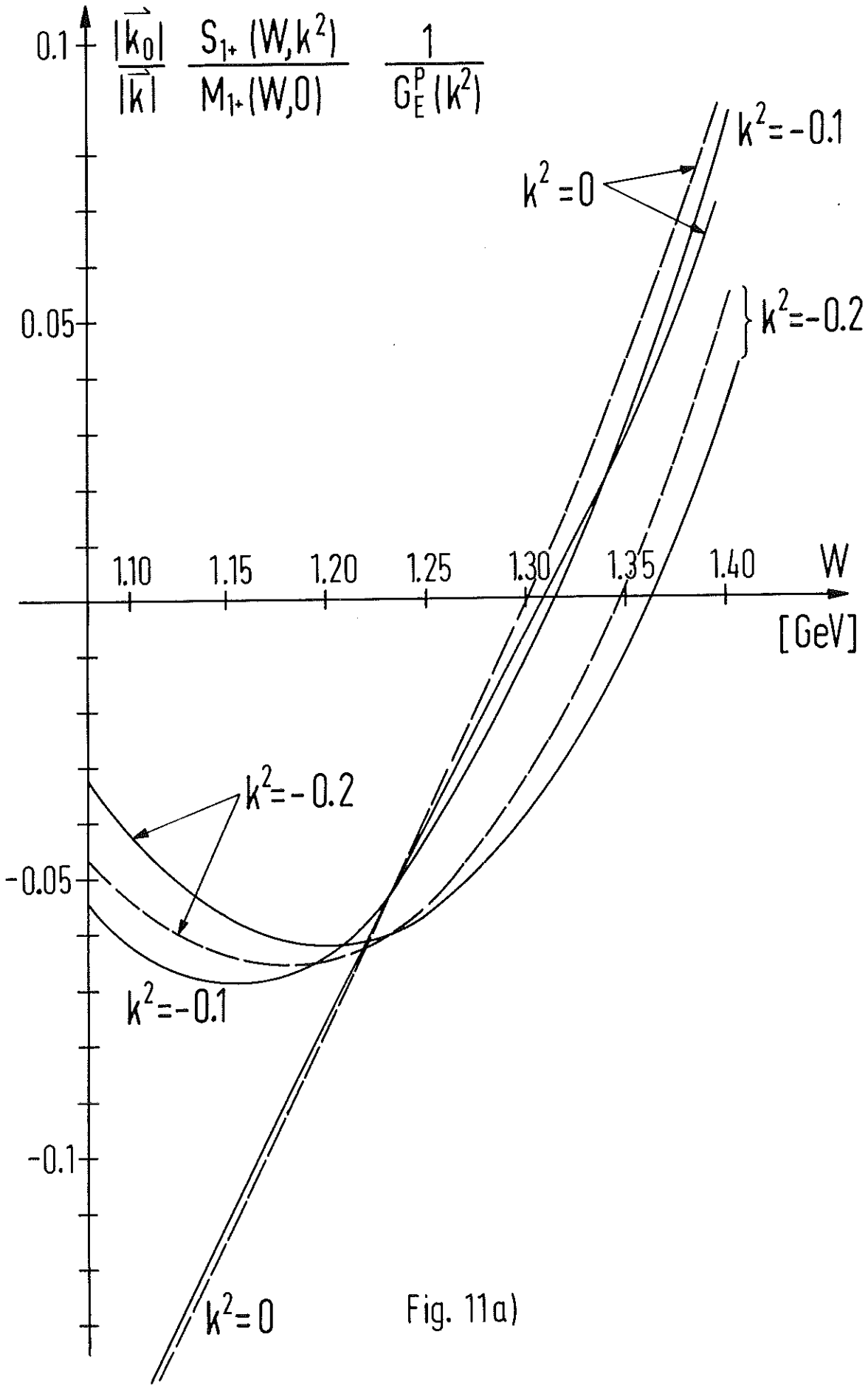
$\frac{|\vec{k}_0|}{|\vec{k}|}\ \frac{S_{1+}(W,k^2)}{M_{1+}(W,0)}\ \frac{1}{G_E^p(k^2)}$
0.1
0.05
-0.05
-0.1
1.10
1.15
1.20
1.25
1.30
1.35
1.40
W
[GeV]
$k^2=-0.1$
$k^2=0$
$k^2=-0.2$
$k^2=-0.2$
$k^2=-0.1$
$k^2=0$

Fig. 11a)

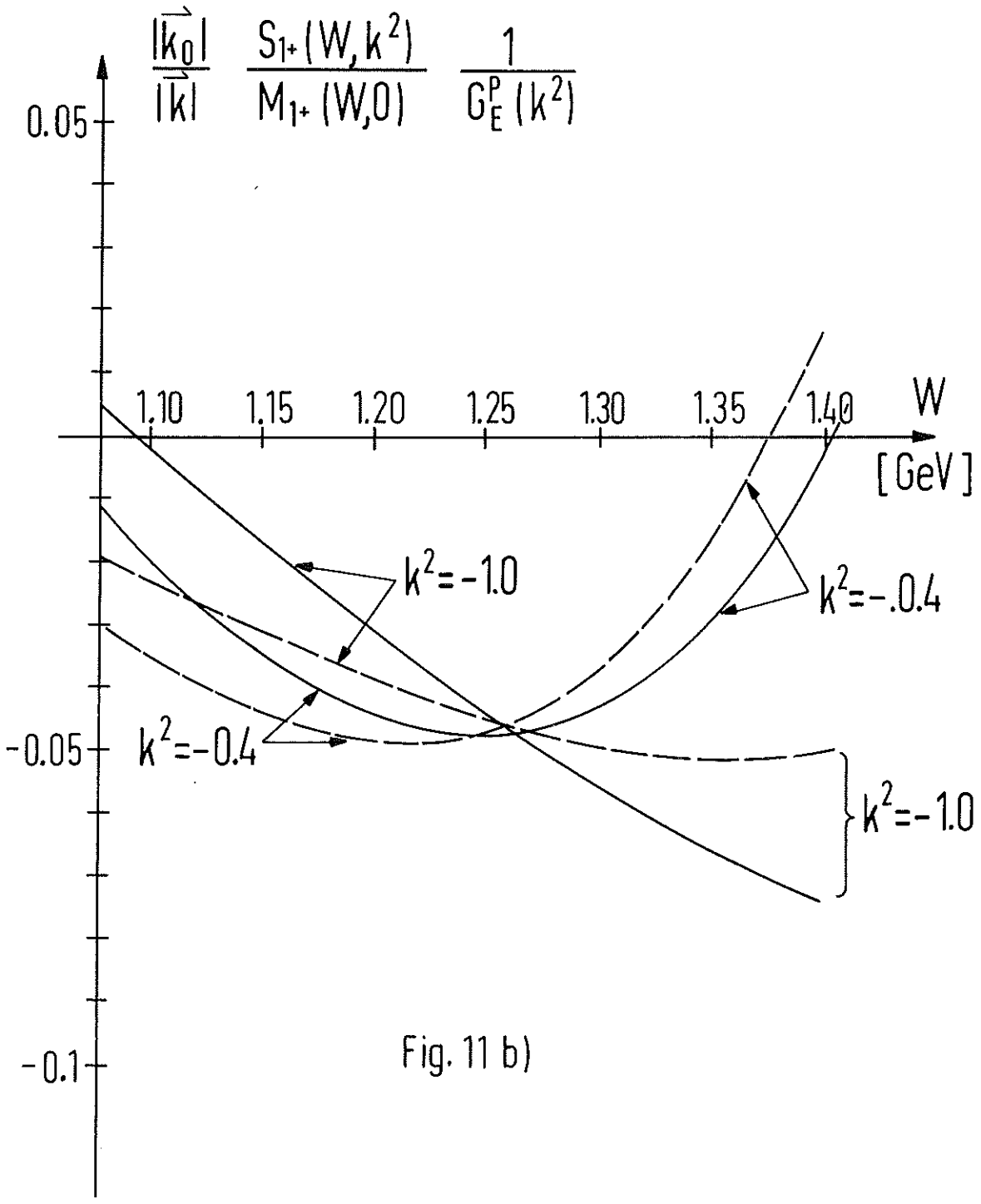
$\frac{|\vec{k}_0|}{|\vec{k}|}\ \frac{S_{1+}(W,k^2)}{M_{1+}(W,0)}\ \frac{1}{G_E^p(k^2)}$
0.05
-0.05
-0.1
1.10
1.15
1.20
1.25
1.30
1.35
1.40
W
[GeV]
$k^2=-1.0$
$k^2=-.0.4$
$k^2=-0.4$
$k^2=-1.0$

Fig. 11 b)